The spatiotemporal organization of experience dictates hippocampal involvement in primary visual cortical plasticity

HHS Public Access

Author manuscript

Curr Biol. Author manuscript; available in PMC 2022 September 27.

Published in final edited form as:

Curr Biol. 2021 September 27; 31(18): 3996–4008.e6. doi:10.1016/j.cub.2021.06.079.

The spatiotemporal organization of experience dictates hippocampal involvement in primary visual cortical plasticity

Peter S. B. Finnie[1], **Robert W. Komorowski**[1,2], **Mark F. Bear**[1]

[1]Massachusetts Institute of Technology, The Picower Institute for Learning and Memory, Department of Brain and Cognitive Sciences, Massachusetts Ave., Cambridge, 02139, USA.

[2]Current affiliation: Biogen Inc., Division of Clinical Development, Binney St., Cambridge, 02139, USA.

Summary

The hippocampus and neocortex are theorized to be crucial partners in the formation of long-term memories. Here, we assess hippocampal involvement in two related forms of experience-dependent plasticity in the primary visual cortex (V1) of mice. Like control animals, those with hippocampal lesions exhibit potentiation of visually evoked potentials following passive daily exposure to a phase reversing oriented grating stimulus, which is accompanied by long-term habituation of a reflexive behavioral response. Thus, low-level recognition memory is formed independently of the hippocampus. However, response potentiation resulting from daily exposure to a fixed sequence of four oriented gratings is severely impaired in mice with hippocampal damage. A feature of sequence plasticity in V1 of controls, but absent in lesioned mice, is generation of predictive responses to an anticipated stimulus element when it is withheld or delayed. Thus, hippocampus is involved in encoding temporally structured experience, even within primary sensory cortex.

Keywords

primary visual cortex; hippocampus; synaptic plasticity; long-term memory; systems consolidation

Introduction

Distinctions between hippocampus-dependent and -independent memories may include the locus of information storage, the types of information stored, and the mechanism(s) of encoding and consolidation[1–5]. In recent years it has been established that mouse primary visual cortex (V1) is a storage site for several types of memory historically considered

Lead Contact: Mark Bear, Department of Brain and Cognitive Sciences, Massachusetts Institute of Technology, Cambridge, MA, USA 02139 mbear@mit.edu.

Author contributions.

Conceptualization, P.S.B.F., R.W.K., and M.F.B.; Methodology, P.S.B.F., R.W.K, and M.F.B.; Formal Analysis, P.S.B.F. and R.W.K.; Investigation, P.S.B.F. and R.W.K; Writing - Original Draft, P.S.B.F. and M.F.B.; Writing - Review & Editing, P.S.B.F., R.W.K., and M.F.B.; Visualization, P.S.B.F.; Supervision, P.S.B.F. and M.F.B.; Project Administration, P.S.B.F. and M.F.B.; Funding Acquisition, P.S.B.F. and M.F.B.

Declaration of interests.

The authors declare no competing financial interests. RWK is currently an employee of Biogen, Inc.

to be the domain of “higher” brain regions[6], offering a new opportunity to understand the nature of hippocampus-dependent encoding in neocortex. The advantages of studying mouse V1 are that (1) sensory experience can be precisely controlled, (2) experience-dependent plasticity is reported by robust changes in visual-evoked potentials (VEPs), and (3) modifications can occur prior to binocular integration and depend on mechanisms local to V1, therefore pinpointing this as a critical locus of storage[7]. However, it remains to be established if any of these experience-dependent modifications of V1 depend on hippocampus, and if they do, what distinguishes them.

In the current study, we have compared the hippocampal dependence of two similar forms of V1 plasticity. Both are triggered by brief daily exposure of awake head-fixed mice to carefully controlled visual stimuli, and generate potentiated VEP responses recorded from V1 layer 4 (L4). The first protocol consists of passive exposure to a phase-reversing oriented grating stimulus (parallel black and white bands that swap positions twice per second), which elicits stimulus-selective response plasticity (SRP) expressed as an increase in VEP magnitude recorded in V1[8]. This response modification possesses attributes consistent with perceptual learning, including gradual emergence in the hours following experience, persistence over weeks, and exquisite stimulus selectivity[9,10]. SRP is accompanied by habituation of an innate behavioral response to presentation of the visual grating stimulus, indicating formation of long-term recognition memory[11]. Both the electrophysiological and behavioral measures of memory formation are disrupted by local manipulations of N-methyl-d-aspartate (NMDA)-receptors and inhibitory neurotransmission within V1, suggesting a common mechanistic basis in neocortex[7,12]. The second visual stimulation protocol comprises repeated daily exposure to four distinct grating orientations, arranged in a consistent temporal order. Like SRP, the response potentiation emerges gradually in the hours after stimulation, is highly selective for stimulus properties present during training, occurs prior to binocular integration, and is reliant on plasticity mechanisms local to V1[13]. However, unlike SRP, visual sequence plasticity depends on local activation of muscarinic acetylcholine (mACh) receptors and does not require NMDA-receptors in V1[13]. Thus, SRP and sequence potentiation are similarly expressed by VEPs in V1, but are driven by qualitatively different types of experience and depend on distinct mechanisms.

In the current study we demonstrate that these two similar forms of V1 response potentiation also have dissociable reliance on the hippocampus. In mice with dorsal and ventral hippocampal damage, both SRP and long-term behavioral habituation are largely normal, but V1 potentiation elicited by visual sequence exposure is virtually absent. Control mice familiarized to a consistent sequential pattern of visual stimulation produce anticipatory V1 responses even when an element is omitted or delayed. Hippocampal damage eliminates this generative V1 response, providing evidence that interactions between these regions are necessary for spatiotemporal prediction[14]. Moreover, following daily exposure to a series of gratings, hippocampectomized mice undergo far less potentiation not just to the familiar sequential arrangement, but also when the stimuli are presented in reverse order, suggesting a failure to encode each constituent grating orientation. These findings suggest that the hippocampus contributes to long-term plasticity in primary sensory cortex under circumstances when discrete stimuli are arranged in a predictable temporal order.

Results

Long-term visual recognition does not require the hippocampus.

To assess hippocampal involvement in low-level visual recognition memory we recorded extracellular local field activity from L4 of binocular V1 along with concomitant forepaw movement while head-restrained mice viewed an oriented sinusoidal grating over multiple daily sessions. This protocol includes no reinforcement or explicit associative structure, and stereotyped behavioral and neural response changes emerge as animals adapt to passive visual stimulation. In the standard protocol the grating stimulus is presented in a continuous phase-reversing pattern repeating 1000 times per session, divided among 5 discrete blocks. We use the term “vidget” to describe a reflexive forepaw movement that tends to occur when the visual pattern transitions from gray screen to grating at the start of each block[11]. Electrophysiological VEP responses were measured in L4, given the extensive characterization in prior studies[7] and because this is the cortical depth at which the VEP has maximal negativity in the mouse, reflecting a local current sink[15]. To eliminate hippocampal influences on experience-dependent behavioral and cortical plasticity we applied permanent bilateral lesions prior to experimentation via NMDA nanoinjections into the hippocampus[16]. Figures 1A–B and S1A–B display representative examples of bilateral hippocampal lesions that met inclusion criteria, alongside coronal sections from the brains of littermate control mice that received sham lesions. Post-mortem histology determined that the area of gross residual hippocampal tissue following lesioning was 40.09 ± 9.85% that of sham mice (mean ± SEM = 100 ± 4.34%), a statistically significant difference (Mann-Whitney U = 9, n_{sham} = 11, n_{lesion} = 12, p = 0.0001). In Table S1 we report tests of correlations between estimated residual hippocampal tissue volumes and critical outcome measures collected throughout this study.

Before describing our results, two limitations of the study should be explicitly acknowledged. First, the application of lesions prior to experimentation could conceivably impair the induction, consolidation, and/or expression of behavioral or neural response plasticity. Our experiments therefore do not allow us to specify which phase(s) are affected by the lesions. Second, control mice received sham injections in the hippocampus rather than volume-matched lesions elsewhere in the brain. Thus, we cannot exclude the possibility that it is the amount rather than the locus of tissue damage that accounts for the observed effects. However, the lesion method and controls we employed have been widely used for many years to gain insights into hippocampal function, and therefore are well validated.

Lesion and sham control mice underwent surgery as cohorts on the same day. They recovered from surgery for 14–21 days and then, prior to commencing the SRP protocol, received two daily sessions of acclimation to head-fixation while viewing a uniform gray screen. The following day the mice were exposed to an isoluminant, phase-reversing grating stimulus of a fixed orientation for six consecutive days (Figure 1C–D). On Day 1 (baseline), mean VEP magnitudes were significantly smaller in the lesion (106.1 ± 16.64 μV) relative to sham (187± 33.71 μV) group (two-tailed unpaired t-test, t_{21} = 2.21, p = 0.038), but showed no correlation with residual hippocampal tissue volume (see Table S1). The cause(s) of the baseline response magnitude difference remain unidentified, but

could include altered electrical volume conduction[17], disrupted network synchrony[18–22], histologically undetectable diaschisis within the thalamocortical visual circuit[23], or shifting V1 electrode placement due to atrophy of the underlying hippocampal tissue. Unlike the VEP, V1-dependent behavioral responses to the onset of grating stimuli on Day 1 were comparable in each group (normalized to pre-stimulus baseline; two-tailed unpaired *t*-test, $t_{21} = 1.47$, $p = 0.16$; Figure S1D), as was spontaneous movement during the interleaved presentations of gray screen between blocks (two-tailed unpaired *t*-test, $t_{21} = 1.53$, $p = 0.14$; Figure S1C). There was also no correlation between residual hippocampal tissue volume and Day 1 vidget magnitude in the lesion group (Table S1). Importantly, across the first six days of exposure to the same oriented grating stimulus, VEP magnitudes potentiated significantly with no detectable differences between groups (Figure 1E). Thus, SRP acquisition was normal in mice with hippocampus lesions. On Day 7, the responses to the familiar stimulus were compared to a stimulus with a novel orientation (each normalized to Day 1 responses). In both groups, VEP responses were potentiated for the familiar relative to novel stimulus, but this was significantly exaggerated in lesioned mice (Figure 1F–G). The apparent enhancement of potentiation could be attributable to the smaller baseline VEP magnitudes measured in hippocampectomized mice, or to improved encoding[24–26]. Regardless, an intact hippocampus is evidently not critical for this form of experience-dependent V1 plasticity. Concomitant orientation-selective habituation (OSH) of the vidget was likewise observed in both groups (Figure 1H), which did not differ statistically (Figure 1I). A separate cohort of mice that received lesions targeting only the dorsal hippocampus (dH) likewise acquired and expressed both SRP and OSH at normal levels (Figure S2). Thus, the hippocampus is not required for V1 plasticity underlying long-term visual recognition memory.

To test whether the hippocampus is required for the retention or consolidation of SRP over longer time intervals[27], most mice reported above also received a second test session 10 days following completion of the 7-day protocol (*n*/group: sham = 8; lesion = 9). SRP persisted in both the sham and lesion groups (Figure S1E–G), indicating stable maintenance of plasticity over weeks or more, even when formed in the absence of the hippocampus.

To verify the functional ablation of hippocampus, after completion of the SRP protocol we next subjected all mice to an object displacement behavioral task known to be sensitive to hippocampal dysfunction[28,29] (Figure 2). In both groups, the exploration of two identical objects in static locations diminished significantly across four sampling sessions. However, during a final test session, only mice in the sham condition preferentially explored the object that had been moved to a new spatial location whereas lesioned mice investigated both objects for an equivalent duration. This finding is consistent with bilateral damage to the hippocampus. The volume of residual hippocampal tissue in the lesion group did not correlate with exploration of the displaced object (Table S1) suggesting that all lesions crossed the threshold required to maximally disrupt this type of memory.

Hippocampal damage disrupts potentiation of V1 responses following visual sequence exposure.

Hippocampal perturbations can disrupt the ability to learn the spatial and temporal arrangement of previously encountered items[16,30,31]. Thus, primary sensory cortex alone

may be sufficient to form simple stimulus representations, but relational memory might additionally require the hippocampus[29,32,33]. To investigate this possibility, we interrogated a form of VEP potentiation that is evoked in V1 when mice are exposed daily to gratings of 4 different orientations in a fixed sequence (referred to here as stimulus *A*, *B*, *C*, and *D*; Figure 3A)[13]. As in the prior experiment, mice were pseudorandomly assigned to receive NMDA or sham lesions of hippocampus 14–21 days prior to training. We hypothesized that the lesion group would undergo potentiation comparable to controls in response to the 4 gratings (as observed during SRP), but following training, only sham controls would show additional VEP potentiation when viewing the stimuli in the predictable forward arrangement versus the reverse order. In this experiment, the mean area of residual tissue in the lesion group occupied 35.22 ± 4.85% the total area of control hippocampus (two-tailed unpaired t-test, $t_{11} = 11.67$, $p < 0.0001$), which was both qualitatively and quantitatively comparable to the 40.09% tissue spared in the lesion group from the SRP experiment (two-tailed Mann-Whitney $U = 28$, $n_{SRP} = 12$, $n_{sequence} = 6$, $p = 0.49$). The lesion group exhibited no significant correlations between residual hippocampal tissue area and the major outcome measures in these experiments (Table S1).

As on Day 1 of the SRP protocol, mean baseline VEP magnitudes elicited by the four stimuli in the visual sequence appeared larger in the sham group relative to the lesion group (Figure 3B), although this did not reach statistical significance (two-tailed Welch's *t*-test for unequal variances, $t_{8.42} = 0.73$, $p = 0.485$). There was also no significant linear relationship between residual hippocampal tissue in the lesion group and Day 1 VEP magnitude (Table S1). Across consecutive training days, sham control mice exhibited robust potentiation of mean VEP responses elicited by the stimulus sequence, whereas lesioned mice exhibited no significant change in VEP magnitude (Figure 3B–C). Consistent with conclusions of a prior study[13], the deficit in potentiation was not merely a consequence of reduced VEP amplitude at Day-1 baseline (Figure S3A), as confirmed using multiple linear regression. A model including both group membership (lesion vs sham) and baseline VEP magnitude was a significant predictor of percent potentiation between days 1 and 4 ($F_{2,10} = 18.04$, $p = 0.0005$). Adjusting for Day 1 VEP magnitude (which was not itself a unique predictor; $\beta = -0.149$, SE = 0.137, $p = 0.30$), group membership still significantly explained potentiation across days ($\beta = -133.0$, SE = 22.15, $p = 0.0001$). Finally, analyses restricted to responses elicited by the first element in the sequence (stimulus A) detected no group difference in potentiation across days (Figure S3C–D). Therefore, hippocampal lesions selectively disrupt sequence-evoked plasticity in V1 cued by stimulus A, while leaving SRP intact.

To parse sequence- from stimulus-selective potentiation, on Day 5 mice were exposed to the same set of 4 oriented gratings, presented in both forward (*ABCD*) and reverse (*DCBA*) order. As the first stimulus in the familiar sequence ('*A*') appears to predictively cue neural response modulation to gratings presented thereafter, potentiation is typically most pronounced for the two middle elements[13]. Thus, to assess the effect of hippocampal lesions on V1 plasticity evoked by spatiotemporal patterns we compared VEPs elicited by elements *B* and *C* in the forward and backward sequences, after normalizing to mean Day 1 magnitude for each group (Figure 3D). Comparing BC and CB specifically controls for any differences in potentiation driven by familiarity with the spatial features of the grating stimuli, thus isolating the effects of sequential order. Further, by analyzing the mean of

B and C responses rather than individual VEP magnitudes at each ordinal position (see Figure S3D), we avoid conflating stimulus identity and anticipatory temporal prediction. This analysis reveals that only sham control mice exhibited significant sequence-specific potentiation (greater magnitude of BC vs CB responses), which was absent in the lesion group (Figure 3E–F). Surprisingly, the normalized response magnitude evoked by the reverse sequence (*CB*) was also significantly larger in the sham versus lesion group. This finding suggests that direction-invariant potentiation of VEPs, putatively elicited by familiarity with each discrete oriented stimulus, is absent in hippocampectomized mice—in stark contrast to the supranormal SRP observed in lesioned mice (Figure 1). Multiple linear regression again confirmed that experimental group was a significant predictor of sequence-specific potentiation ($F_{2,10} = 18.04$, $p = 0.0005$; $\beta = -0.467$, SE = 0.151, $p = 0.0001$), over and above the baseline VEP response differences present on Day 1 ($\beta = 0.0003$, SE = 0.0009, $p = 0.777$).

To confirm that hippocampectomy has differential effects on sequence-specific potentiation versus SRP, we compared the ratio of familiar to novel stimulus orientations on SRP day 7, to the ratio of forward and reverse visual sequence elements (stimuli BC vs CB) collected on visual sequence day 5. In the sham condition these ratios were statistically indistinguishable (two-tailed Mann-Whitney $U = 37$, $n_{SRP} = 11$, $n_{sequence} = 7$, $p = 0.93$), whereas in the lesion condition the ratio of stimulus- to sequence-specific potentiation was exaggerated ($U = 3$, $n_{SRP} = 12$, $n_{sequence} = 6$, $p = 0.0008$; Figure S3B). Thus, these two forms of V1 plasticity have dissociable reliance on the hippocampus.

Anticipatory V1 responses are disrupted by hippocampal lesions.

Our findings are consistent with the hypothesis that the hippocampus contributes to temporal patterning[34,35]—modulating V1 response magnitude when cued by the first element in a familiar visual sequence. Previously it has been shown that even when sequence elements are omitted, V1 displays sequential reactivation of spatiotemporal neural response patterns[13,36]. To test hippocampal involvement in this phenomenon, we assessed responses to omitted stimuli using two different approaches.

First, during the Day 5 test session we included a modified version of the familiar forward ABCD sequence in which each grating stimulus was held on screen for 300 ms (twice the standard 150 ms duration). We reasoned that when cued with stimulus A, mice would expect the onset of stimulus B approximately 150 ms later and display an anticipatory response even when a visual transition had not yet occurred. We focused our analyses on responses to N2-P2 components as we lacked *a priori* predictions about whether an internally-generated anticipatory representation of stimulus B at the expected latency would itself modulate responses when the delayed stimulus is finally presented. After 4 prior days of exposure to the ABCD sequence, the N2-P2 components of the field potential that followed presentation of stimulus A were exaggerated in the sham group, suggestive of an anticipatory response at the expected latency for stimulus B (Figure 4A). In the lesion group, this anticipatory response modulation appeared far less pronounced. To determine if this exaggerated response was merely a consequence of the slightly larger VEPs in the sham group, we normalized the N2-P2 magnitude to the preceding N1-P1 components evoked by stimulus

A (which should exhibit minimal predictive modulation). Even after normalization, sham control mice displayed significantly larger anticipatory N2-P2 responses prior to the delayed onset of stimulus B (Figure 4C). A multiple linear regression model further confirmed that group membership was a significant predictor of normalized N2-P2 magnitude during stimulus B delay trials ($F_{2,10} = 20.82$, $p = 0.0003$; $\beta = -42.92$, SE = 6.774, $p < 0.0001$) after adjusting for Day-1 baseline VEP magnitudes ($\beta = 0.0032$, SE = 0.0696, $p = 0.965$).

Although the potentiated N2-P2 response in sham mice may reflect an anticipatory response, another possible interpretation is that these components are typical long-latency features of the VEP that occur when a familiar grating is not interrupted by another stimulus 150 ms later. If this were the case, then mice with hippocampal damage might simply possess impaired long-latency VEP responses. To investigate this possibility, we quantified the trough-to-peak N2-P2 magnitude elicited by the familiar stimulus on Day 7 of the SRP protocol (re-analyzed from Figure 1), in which there is no expectation of stimulus B at the typical latency of the N2-P2 components. As hypothesized, we found that N2-P2 response magnitudes (normalized to the preceding N1-P1 VEPs) were comparable in sham and lesion groups (Figure 4B–C), indicating that hippocampal damage does not impair the generation of long-latency evoked responses within the SRP protocol. We also found that the latencies of N2 and P2 responses in both groups are not significantly altered by the delay of stimulus B (Figure S3E-F). Thus, we conclude that while mice with hippocampal damage are able to generate typical late components of the VEP, they possess a deficit in cued anticipatory modulation of V1 responses following daily adaptation to visual sequences.

Next, to further assess anticipatory response generation in V1, on experimental day 10 we again presented the familiar sequence ABCD along with a variant in which gray screen was substituted for stimulus B (A_CD)[13]. In sham control mice we confirmed that presentation of stimulus A led to the generation of large amplitude N2-P2 responses at the time when stimulus B was anticipated, even when the grating was omitted (Figure 4D–G). In contrast, the lesion group displayed neither significant response potentiation when comparing the VEPs elicited by stimulus B on Days 1 and 10, nor an anticipatory response during gray screen when cued by stimulus A. On Day 10 the N2-P2 responses in lesion mice were also significantly larger when stimulus B was presented versus omitted, further suggesting a failure to “fill-in” the predictable oriented grating following hippocampal damage. As a direct comparison of predictive response modulation between groups, mice with hippocampal lesions likewise displayed significantly smaller VEPs to gray screen when normalized to their response to stimulus B on Day 10 (Figure 4H). To confirm that systematic differences in Day-1 VEP magnitude did not account for the observed group N2-P2 response differences on Day-10 omission trials, multiple linear regression was performed as described previously ($F_{2,10} = 20.82$, $p = 0.0003$). Although Day 1 VEP magnitude was itself a negative predictor of normalized response magnitude during the omitted stimulus ($\beta = 4.323$, SE = 0.755, $p = 0.0002$), after accounting for this baseline difference group assignment remained a significant predictor ($\beta = -310.0$, SE = 73.49, $p = 0.0018$). Finally, as reported for responses during the delay of stimulus B on Day 5, in the sham group stimulus B omission on Day 10 did not significantly shift the latency of N2 or P2 responses. In the lesion group the P2 latency was also not significantly shifted during omission versus inclusion trials, although the peak N2 response was slower when stimulus B was presented

as predicted than when it was omitted (Figure S3G–H), suggesting a loss of temporal precision of any residual plasticity. Together, these findings are consistent with a specific role for hippocampus in predictive response generation during exposure to familiar temporal patterns of visual stimulation.

Distinct VEP modulation by stimulus familiarity versus spatiotemporal prediction.

We have inferred a role for hippocampus in spatiotemporal encoding because lesions impaired sequence-evoked plasticity, but not SRP. In part, this interpretation rests on the assumption that SRP principally reflects familiarity with the spatial characteristics of an oriented grating stimulus[11], but not the temporal properties of training. However, like the sequence protocol, the visual stimulation pattern used to induce SRP also possesses a stereotyped temporal structure (typically 2 Hz phase reversals). Thus, SRP might likewise involve spatiotemporal prediction. Consistent with this idea, SRP expression possesses emergent properties, manifesting not at the onset of a train of familiar visual stimuli but rather on subsequent phase reversals[37–39]. If SRP were revealed to be strongly dependent on temporal characteristics of visual experience (as it is for spatial features[40]) this would challenge our interpretation that hippocampal lesions selectively disrupt sequential pattern completion. To clarify whether SRP reflects familiarity with stimulus identity or anticipatory prediction of a temporal pattern, a cohort of neurotypical mice was exposed daily to a static grating stimulus at a fixed spatial orientation. After 6 days of exposure, SRP was tested by presenting the familiar stimulus along with a novel orientation (in interleaved blocks), each phase-reversing at 2 Hz to evoke time-locked responses (Figure 5). Even though the experience during training did not entail strong synchronous V1 activation triggered by phase reversals, robust VEP potentiation was still observed following passive daily exposure to a static grating stimulus. These results demonstrate that SRP does not depend on a predictive response for each upcoming phase reversal in a temporal pattern, and familiarity with a given grating orientation may instead engage a sustained processing mode that modulates responses for incoming stimulus transitions[38].

Finally, to determine whether spatiotemporal prediction enhances potentiation beyond what would be expected from stimulus familiarity alone, we next integrated the critical features of SRP and visual sequence patterns into a single protocol. Mice viewed two different pairs of gratings during each daily recording session (one consisting of phase-inverted stimuli at the same spatial orientation, the other consisting of two stimuli at distinct orientations). Response potentiation was exaggerated for the second element in the orientation-shifted relative to the phase-shifted pair (Figure 6). This finding indicates that an expected shift in stimulus orientation confers additional anticipatory response modulation on top of the sustained potentiation triggered by stimulus recognition.

Discussion

Previous studies established that synaptic modifications essential for both SRP and sequence plasticity reside specifically within V1[6,7], but the possibility of hippocampal involvement was unknown. We found that SRP and the associated long-term behavioral habituation to stimuli recognized as familiar occur independently of the hippocampus. In sharp contrast,

hippocampal ablation severely disrupted potentiation of VEPs elicited by a specific sequence of oriented gratings viewed repeatedly across days. Thus, the hippocampus appears to support some forms of long-term experience-dependent plasticity within V1, contingent on the precise spatiotemporal structure of visual stimulation.

At first pass, our data are consistent with the notion that the hippocampus is important for relational memory by indexing stimulus representations stored in V1[33,41]. A classical taxonomy of long-term memory systems posits that neocortical plasticity alone can support low-level mnemonic operations like sensory priming and perceptual learning, whereas the hippocampus is additionally required to encode declarative information, including episodic memory[4]. In non-human animals, "episodic-like" memory has often been approximated using spatiotemporal tasks that capture defining phenomenological features (i.e. the ability to recall when *and* where a specific item has been encountered)[35,42]. For instance, rodents with hippocampal damage can often learn the identity of objects encountered as they explore an environment, but not their relative positions in space and/or time[43–45] (Figure 2). Our findings collected via V1 electrophysiological recordings largely support this distinction. During SRP, stimulus representations appear to be encoded in such a manner that they are dissociable from their surrounding spatial and temporal context[11] (Figure 5). However, when multiple grating stimuli are arranged in a consistent sequential pattern, the resultant V1 potentiation is impaired by hippocampal ablation. As sequence-specific potentiation is eye-specific and requires local plasticity mechanisms in V1[13], a simple model is that sensory neocortex stores the identity of low-level stimuli locally and recruits the hippocampus to preserve the temporal relationships among them[31]. This is consistent with theories positing that the hippocampus does not form a complete, independent record of sensory experience, but rather encodes temporally structured experience by indexing discrete stimulus features stored in neocortex[46]. Indeed, anticipatory response modulation within a familiar sequence inherently involves pattern completion (the ability to retrieve a complete record of sensory experience when provided a subset of the original cues), which has been attributed to autoassociative network properties conferred by the anatomical connectivity of the hippocampus[34,47,48].

Although the cortico-hippocampal index model is intuitively appealing, our findings raise an interesting caveat. An implicit assumption of the model is that neocortex encodes discrete stimulus representations while the hippocampus is necessary to form associations among them (at least initially following experience). Thus, the theory assumes that the neural representation for a given visual stimulus will be stored in essentially the same way by V1 regardless of the preceding and subsequent sensory input. However, at the mechanistic level this is clearly not the case. Blocking activity of NMDA-receptors prevents SRP induction but has little effect on sequence-specific potentiation[13]. Conversely, blocking muscarinic acetycholine receptors locally in V1 disrupts sequence-specific potentiation but has little effect on SRP. Thus, there exist in V1 distinct molecular mechanisms capable of achieving precise orientation-selective stimulus encoding, and these may be differentially recruited and/or modulated by the hippocampus. Distinct encoding mechanisms could explain our puzzling finding that mice with hippocampal lesions show significantly less VEP potentiation than the sham group when stimuli are presented in the reverse sequence on test day (Figure 3E). It appears as though hippocampectomized mice fail to modulate cortical

responses to each discrete familiar stimulus specifically when these had been arranged in a sequential pattern throughout training, even though V1 potentiation and behavioral habituation are both normal in the SRP protocol (Figure 1). Therefore, how the brain stores long-term representations of individual oriented gratings appears to vary depending on their relationship to other sensory stimuli. This conclusion is consistent with observations that neocortical representations of sensory stimuli are strongly influenced by other environmental cues, such as spatial position[49], and that this modulation requires the hippocampus[50]. One compelling model is that the hippocampus specifically encodes so-called successor representations that preserve relationships or transitions among sensory features[51] rather than the identity of each discrete stimulus.

Accounting for how the hippocampus might selectively modulate VEPs elicited by sequential visual stimuli (but not individual gratings) warrants an overview of the intracortical and systems mechanisms known to contribute to these distinct forms of V1 plasticity. Although neural recordings during both protocols were performed in L4—the major recipient layer of monocularly-segregated feedforward visual input in mouse V1—it is important to recognize that VEP magnitude reports more than a change in strength of thalamocortical synapses[9]. Indeed, although there is evidence that SRP induction and maintenance depend upon mechanisms shared with long-term potentiation in V1[40], available data suggest that expression of VEP plasticity in layer 4 is primarily explained by the differential recruitment of inhibitory interneurons by familiar and novel stimuli[12,38]. How these findings fit together is the subject of ongoing investigation, but it is clear that familiar and novel stimuli differentially recruit polysynaptic circuits. Indeed, as SRP is not expressed at the onset of a block of stimulation, but only after the first phase-reversal[37,38], there is ample time for feedback modulation that could even include changes in the mode of transmission through the lateral geniculate nucleus.

The local circuits and brain systems involved in V1 plasticity in response to visual sequences are even less well defined. Like SRP, sequence-specific potentiation occurs prior to binocular integration in V1 and is parsimoniously explained by modification of eye-specific, geniculocortical synaptic transmission[13]. However, it is notable that in L4 the magnitude of the short-latency N1 response elicited by stimulus A in the forward ABCD sequence does not discernably change over days of exposure (see Figure S3C–D caption for statistics). Thus, just as for SRP, thalamocortical synaptic plasticity outside of L4 is a likely site of modification essential for expression of eye- and sequence-specific potentiation of the VEP. Plasticity in other thalamorecipient layers (e.g., L6) conceivably could trigger polysynaptic modulation of the VEP response in L4 for the cued elements ‘BCD’ of the familiar sequence. In principle, this modulation could involve long loops involving hippocampus and intermediary cortical regions. However, the observations that sequence-specific potentiation is (1) eye-specific and (2) blocked locally by inhibition of mACh receptors[13] strongly suggest the essential synaptic modifications occur within V1. These properties challenge popular models in which predictions based on sensory experience are stored in hippocampus and higher visual regions and then transmitted back to V1 to modulate low-level sensory processing[49,52,53]. Our findings are more compatible with a model in which information is stored locally in V1 and used to engage feedback to modulate responses based on learned predictions. In the context of long-loop modulation, an

interesting bridge between hippocampus and V1 is the anterior cingulate cortex[54–56], which was recently shown to express sequence-specific VEP potentiation[57]. However, genetic and pharmocogenetic manipulations showed that anterior cingulate cortex is not obligatory for either induction or expression of sequence-specific potentiation in V1[57].

The question remains as to how the hippocampus might be involved in sequence-specific plasticity. A clue might be the additional requirement of cholinergic transmission in V1. The hippocampus has robust indirect control over the activity of basal forebrain nuclei[58–60], which send cholinergic projections throughout the brain including V1[61]. Acetylcholine typically increases cortical gain, and can both modulate ongoing neuronal responses to patterned sensory input[62–64] and contribute to encoding of stimulus timing by changing the strength of recently active synapses[65]. A recent network model using biophysically realistic synaptic learning rules has shown how precise spatiotemporal sequences can be stored locally in V1 when pulsatile release of a global neuromodulator (putatively acetylcholine) marks the time of experiences that are novel during learning[66]. Thus, one interesting possibility is that the hippocampus is crucial for novelty detection and the consequent activation of the cholinergic basal forebrain. In any case, an important future objective will be to identify the intermediary regions that are essential to bidirectionally transmit modulatory signals between V1 and the hippocampus.

It is worth reiterating that limitations on the interpretation of this study are imposed by our use of permanent lesions. One issue concerns the inclusion of sham controls rather than volume-matched lesions, conceding the possibility that extensive brain damage alone (irrespective of location) could contribute to the observed deficit. Furthermore, functional compensation by other brain regions could occur with prolonged recovery from hippocampal lesioning[67,68]. We also cannot conclusively dissociate the specific contributions of the hippocampus in the acquisition, consolidation, retrieval, and/or expression of visual sequence potentiation. Nevertheless, the current findings address hypotheses on the roles of hippocampus in the storage of information via synaptic plasticity in V1, particularly with regard to consolidation. First, the observation that SRP persists over many days in lesioned animals confirms that not all long-lasting forms of neocortical information storage require hippocampus to be consolidated. Second, although sequence-specific potentiation in V1 is absent in lesioned mice, the properties of this type of plasticity challenge traditional theories of hippocampal involvement in “systems” consolidation. A prevailing view is that rapid plasticity in the hippocampus temporarily stores ongoing experiences until slower intracortical plasticity can gradually strengthen sparse connections among discrete functional ensembles[47,69–71]. Available evidence suggests this handoff from hippocampus to neocortex is achieved by spontaneous reactivation of neural activity patterns during offline rest periods[70,72–75]. However, if this happens in the case of sequence-specific potentiation in V1, it must occur over a far more rapid time-course than is traditionally assumed. A single exposure to novel visual sequences over ~10 minutes leads to sizeable and stable VEP potentiation that is nearly asymptotic 1 day later (Figure 3C). Furthermore, the offline reactivation of visual sequences stored in hippocampus alone seems unlikely to drive sequence-specific response potentiation in V1, as it is difficult to imagine how this could preserve eye-specificity[13].

In conclusion, we demonstrate that long-term neocortical plasticity emerging in the hours following experience can—for some forms of passive sensory stimulation—depend on the hippocampus. Our results are broadly consistent with classical divisions of mnemonic function across brain regions, with V1 storing local representations of low-level visual stimuli and the hippocampus participating in the encoding of higher-order relationships among multiple items. When cued by an initial sequence element, V1 exhibits anticipatory responses even when the subsequent stimulus is withheld, strongly indicative of spatiotemporal pattern completion. Indeed, it has been posited that the hippocampus yields a generative model of upcoming sensory input based on patterns encountered in the past, which provides predictive feedback to earlier sensory cortices[14]. However, our data also suggest that the brain may not store discrete elements of sequential experience in modular fashion, but rather as conjunctive representations of the stimuli as embedded within their temporal context[76]. The well-controlled, passive visual stimulation protocols and robust electrophysiological reports of V1 plasticity described here provide a powerful platform to further delineate when and how the hippocampus contributes to neocortical encoding, storage, and retrieval of visual experiences.

STAR Methods.

RESOURCE AVAILABILITY.

Lead contact.—Further information and requests for resources and reagents should be directed to and will be fulfilled by the lead contact, Mark Bear (mbear@mit.edu).

Materials availability.—This study did not generate new unique reagents or organisms.

Data and code availability.—All code for generation of visual stimuli and data analysis is as described in prior studies[11,13], and is accessible via github repository (github.com/jeffgavornik/VEPAnalysisSuite; github.com/jeffgavornik/VEPStimulusSuite). The datasets supporting the current study (including electrophysiological and behavioral recordings during visual stimulation) are publicly available via Mendeley Data: https://doi.org/10.17632/sspngbxbcz.1

EXPERIMENTAL MODEL AND SUBJECT DETAILS.

All subjects were male C57BL/6N mice obtained from Charles River Laboratory International (Wilmington, MA; RRID:MGI:5651595) at postnatal day 25–26 (P25–26). At the time that this study was conducted only male mice were used due to evidence of distinct behavioral patterns in females, which are not adequately captured using our established assay of visually-evoked forepaw responses in head-restrained mice. This major limitation is being systematically addressed in the context of ongoing studies. After arriving at MIT, mice were housed in groups of 2–5 littermates on a 12h dark-light cycle (light phase beginning at 7:00 a.m.) with food and water provided *ad libidum*. Nalgene homecages contained woodchip bedding and cotton nesting materials. All procedures adhered to the guidelines of the US National Institutes of Health and were approved by the Committee on Animal Care at MIT (Cambridge, MA, USA). All efforts were made to minimize pain or distress in the animals. Data reported is from experimentally-naïve animals except for the object

displacement task, which provided an internal control for cohorts that previously underwent the electrophysiological recordings summarized in Figure 1.

METHOD DETAILS.

Surgical procedures.

General surgical preparation.: Surgeries were performed at P28–30 (except for the experiment in Figure 5, which were performed at P35). Anesthesia was induced and maintained with inhaled isoflurane (1.5–3% in oxygen). Pre-operative subcutaneous injections of meloxicam (1 mg/kg) were administered as analgesic. Body temperature was maintained at 37°C with a heat source positioned under the torso of the mouse. Ophthalmic ointment was applied topically to both eyes to prevent damage. The scalp was shaved and cleaned with providine solution (10% w/v) followed by ethanol (70% v/v), and lidocaine hydrochloride (1%) was injected subcutaneously under the scalp as a local anesthetic. A 1 cm-long midline scalp incision was applied with surgical scissors to reveal an area of skull between the eyes and ears. To improve cement adhesion the skull surface was then carefully cleaned with saline, scored with a scalpel blade, and dried with compressed air. All mice went on to be implanted with local field electrodes. At the completion of all surgical procedures, mice were placed in a recovery chamber with free access to a heat source until the mouse regained consciousness and resumed grooming. In the lesion experiments, all mice received subcutaneous injections of warmed sterile Ringer's solution to aid in recovery. Mice received daily subcutaneous meloxicam (1 mg/kg) injections as analgesic for 48–72 hours following surgery, and were monitored for signs of discomfort or illness. Mice were permitted 14–21 days of post-operative recovery before commencing visual stimulation protocols.

Hippocampal excitotoxic lesions.: The lesioning protocol was adapted from previous studies[16] through extensive pilot testing. Mice were prepared according to the general surgical procedures described above, then mounted on a stereotaxic apparatus (Kopf Instruments) with earbars. The pitch of the skull was adjusted such that bregma and lambda were level with the horizontal plane. A pulled glass pipette was backfilled with mineral oil and mounted on a nanoliter injector (Nanoject III, Drummond Scientific), then front-loaded with either freshly dissolved NMDA solution (#M3262, Sigma-Aldrich; 10 mg/mL in sterile physiological saline [0.9% w/v]) in the Lesion condition, or an equal volume of sterile saline in the Sham control condition. Nano-infusions were targeted at 4 stereotaxically-determined sites per hemisphere, relative to bregma: 1) A/P −1.8mm, M/L +/− 1.3mm, D/V (from dural surface above injection site) −1.4mm; 2) A/P −2.3mm, M/L +/−1.8mm, D/V (from dura) −1.6mm. To minimize the likelihood of damaging V1, for the two injections per hemisphere targeting ventral hippocampus the pipette was angled at 20 degrees, progressing ventrocaudally. Target coordinates for these sites were adjusted to compensate for the angle of approach: 3) A/P −1.8mm, M/L +/− 2.9mm, D/V (from dura) −2.6mm; 4) A/P −1.8mm, M/L +/− 2.9mm, D/V (from dura) 3.2mm. Mice assigned to undergo lesioning restricted to dorsal hippocampus (Figure S2) received injections at only the first 2 sites described above. Tissue was permitted to decompress for 5 minutes after lowering the injector to the desired depth before commencing injections. At each of the first 3 sites 70 nL was injected per hemisphere, in 7 × 10 nL pulses at a rate of 43 nL/sec with 30 seconds between each

pulse. At the fourth injection site 100 nL was delivered in 10 pulses per hemisphere. During infusions dura was kept moist by applying sterile saline to each craniotomy. The pipette was retracted 5–7 minutes following the final pulse at each site, and the craniotomy was sealed with a small bead of Kwik-Sil silicone adhesive (WPI Inc.). Following the final infusion, diazepam was injected subcutaneously (5 mg/kg) as an anticonvulsant to reduce propagation of seizure activity during post-operative recovery after removal of isoflurane.

Electrode implantation.: Extracellular local field potential (LFP) electrodes were implanted following the surgical procedures described above. A steel headpost was affixed between the eyes anterior to bregma using Krazy Glue (Elmers) followed by Loctite 454 cyanoacrylate adhesives. A dental drill was used to apply <0.5 mm craniotomies over frontal/motor cortex in the right hemisphere, and bilaterally over the binocular zone of V1 (+/− 3.1 mm lateral of lambda). A custom-fabricated silver wire (A-M systems, Sequim, WA, US) electrode was positioned approximately A/P +0.5mm, M/L + 1.0mm from bregma, and inserted to a depth D/V −0.3mm onto the surface of frontal cortex to serve as reference. Blunt tapered tungsten microelectrodes (300–500 MΩ, 75μm diameter; #30070, FHC, Bowdoinham, ME) were gradually advanced into binocular V1 to a depth of 450–470 um from dura, targeting layer 4. Electrodes were secured with cyanoacrylate glue, followed by application of Ortho-Jet dental acrylic (Lang Dental, Wheeling, IL, USA) to adhere to the skull surface. An adhesive accelerant (Zip-Kicker, Pacer Technologies, Ontario, CA, USA) was applied sparingly to expedite curing of cyanoacrylates.

Visual stimulation.

Grating stimuli.: During all experimentation the investigators remained blind to group assignment. Visual stimulation and electrophysiological recordings were performed in one of two adjacent enclosed rooms, which remained dimly-lit throughout while preparing each animal and throughout experimentation. To avoid disruption of the circadian cycle by daily visual stimulation, experiments were performed during the 12-hour light phase. Ambient room temperatures maintained between 19–24°C. Awake, head-fixed mice were positioned with eyes 20 cm from the midline of a gamma-corrected LCD display. In one recording suite, the head fixation apparatus and monitor were both contained in a custom sound- and light-attenuating chamber coated on all external sides with grounded copper to minimize electrical noise. Internal walls of the chamber were matt black to reduce light reflections. In the second suite, the equipment was not enclosed within a chamber, but was well grounded away from sources of light, sound, and electrical interference. The second recording suite was used only for the visual sequence experiment due to technical issues on the primary system at the outset of recording. Although we cannot rule out the possibility that the hippocampus is required for V1 plasticity only in one room but not the other, the patterns of visual stimulation may better account for the reported results. SRP and visual sequence protocols have each been performed extensively in both suites in dozens of prior experiments, and the observed plasticity patterns tend to be nearly indistinguishable. In both rooms, custom MATLAB software (RRID:SCR_001622) built around the PsychToolbox extension (RRID:SCR_002881) was used to display full-field visual stimuli (github.com/jeffgavornik/VEPStimulusSuite). After recovery from surgery, mice were acclimated to head restraint in front of a 50% gray screen for 30 minutes on

each of 2 days. The following day a binocular visual stimulation protocol was initiated, consisting of exposure to luminance-defined sinusoidal grating stimuli (100% contrast, 0.05 cycles per degree) arranged in phase-reversing and/or sequential patterns (described below). The orientation of each stimulus was offset by at least 15° from the cardinal angles and 30° from all other stimuli: 15°, 45°, 75°, 105°, 135°, and 165°. Mice were placed in the head restraint apparatus 5 minutes prior to the beginning of each recording session, during which time an isoluminant gray screen was presented.

SRP/orientation-selective behavioral habituation protocol.: In the standard SRP protocol, mice viewed an oriented grating that phase reversed every 0.5 s (2 Hz). Daily for 6 days, mice viewed five blocks of 200 phase reversals interleaved by 30-sec presentations of isoluminant gray screen stimuli. During a SRP testing session (day 7), mice viewed gratings at both the familiar orientation and also a novel orientation (non-cardinal and 90° offset from previously-presented stimuli). Five blocks of each orientation were presented in pseudorandom order (no stimulus was presented for more than two consecutive blocks). A majority of mice reported in Figure 1 were also retested on day 17, during which the familiar stimulus (X°) was presented along with a second novel orientation.

In the static grating experiment, all mice viewed 6 × 100-sec blocks of a single grating orientation on days 1–6 of SRP induction, presented as static images of each phase-inverted phase (3 blocks of each). On the experimental day 7, two distinct orientations were each presented in a 2 Hz phase reversing pattern, including a novel orientation and the familiar orientations viewed over prior days. Both were presented in 3 interleaved blocks of 200 phase reversals.

Visual sequence protocol.: On days 1–4 of the visual sequence protocol, a contiguous series of 4 oriented grating stimuli was repeated 200 times per day in a consistent spatiotemporal order. Individual sequence presentations were interleaved by 1.5-sec intervals of isoluminant gray screen, and arranged into 4 blocks of 50 repetitions interleaved by 30-second gray screen intervals. On test day (day 5), mice viewed 4 blocks of the same sequence in both forward and backward arrangements, as well as the forward sequence presented at 50% temporal frequency (each stimulus held for 300 ms, 1.5s interleaved gray screen). The order of blocks was pseudorandomly shuffled, such that no sequence was viewed more than twice consecutively. Another test session was presented 5–7 days later (experimental day 10), during which the familiar ABCD pattern was presented at the standard temporal frequency, as well as the same sequence with stimulus B omitted (A_CD). Only the first two stimuli (A and B) in the 50% temporal frequency and A_CD omission conditions were analyzed here. The specific grating orientation assigned to each position in the sequence was counterbalanced across mice.

Integrated SRP/Sequence protocol.: To align the stimulation parameters used in the SRP and sequence protocols, in a modified paradigm, individual mice were presented with two pairs of stimuli: one pair phase-inverted gratings of the same orientation (‘Flip’ and ‘Flop’), and the other two distinct grating orientations (‘A’ and ‘B’). The other parameters were adopted from the visual sequence protocol. Specifically, each stimulus was held on screen for 150 ms, with 1.5 sec gray screen stimuli presented between each pair. Four blocks of

each stimulus pair were presented in pseudorandom order, with 30-sec gray screen periods interleaved. Only the plasticity induction sessions (Days 1–4) are reported.

Electrophysiological recordings.: Two electrophysiology systems (Recorder-64, Plexon Inc., Dallas, TX, US) were used to record neural LFP activity in awake, head-restrained mice throughout the multi-day visual stimulation protocols described above. Although these systems are comparable, the absolute magnitude of evoked responses recorded on each cannot be directly compared due to differences in amplifier configuration. Nevertheless, relative differences on each system can be compared (i.e. VEP potentiation, relative magnitudes of distinct VEP components, etc), and each cohort of mice was tested only on one system throughout experimentation. Continuous extracellular voltage signals were collected bilaterally from V1 (referenced to the frontal electrode), low-pass filtered at 500Hz, and digitized at 1000 Hz. All data were analyzed with custom code written in MATLAB (github.com/jeffgavornik/VEPStimulusSuite). To extract visually-evoked potentials (VEPs), the 300–500 ms interval following each stimulus presentation was extracted and averaged across all trials within a block, or in some cases for specific trials across multiple blocks. VEP magnitude was generally defined as the voltage difference between the first negative-going (N1) trough following stimulus onset (~40 ms latency), and the subsequent positive going (P1) peak (typically occurring at a latency of between 60–125 ms). In Figure 4A–C, the subsequent N2 and P2 VEP components were also extracted, and the trough-to-peak magnitude was normalized the magnitude of the preceding N1 to P1 response to stimulus A. An automated detection algorithm was used to measure magnitudes, but each VEP was manually inspected to ensure consistent identification across experimental conditions. The automated detection algorithm detected the minimum voltage value within post-stimulus latency window between 25 and 100 ms (early negative-going component, i.e. N1), and the subsequent peak positive voltage value occurring between the identified latency and 175 ms (subsequent postitive-going component, i.e. P1). The same procedure was used to measure VEP magnitudes in the sequence-exposure protocol, with care taken to ensure that the positive-going component did not overlap with the evoked period of the subsequent stimulus. In the visual sequence paradigm, VEPs were averaged across each of the four stimuli (“ABCD”) when comparing response changes over days. However, generally the first stimulus in the sequence shows comparatively limited response modulation as a function of familiarity, and cues anticipatory potentiation only for subsequent stimuli. Thus, to assess the effects of lesions on long-term plasticity, for the Day 5 test session we opted to compare only responses to the stimuli in positions 2 and 3 of each sequence (orientations B and C) normalized to the ‘baseline’ magnitude for each mouse recorded on Day 1. Likewise, in the integrated SRP/sequence protocol, only the responses to the 2^{nd} stimulus in each phase- or orientation-shifted pair were compared between conditions. The second sequence element was also specifically measured in the temporal delay ($ABCD_{300ms}$) and stimulus omission (A_CD) experiments (Figure 4). Here the analysis was focused on stimulus B rather than averaging the responses to stimulus B and C, in order to isolate the effects of spatiotemporal prediction. This is because modulation of responses to stimuli that follow a withheld element could be influenced both by forward prediction (based on the internally-generated stimulus representation) and prediction error, which are not disambiguated. The latency of responses in the delay/omission tests was measured from the onset of stimulus B in the standard

sequence (beginning after 150 ms exposure to stimulus A). The latency to peak negative going (N2) and positive-going (P2) components was quantified separately for each mouse, and are the same time-points used to determine VEP magnitudes.

Although electrodes were implanted bilaterally, recordings from only one hemisphere of each mouse were included in the final datasets. For each mouse, the chosen hemisphere was selected on the basis of the mean VEP with the largest mean magnitude on Day-1, and possessing morphology consistent with V1 layer 4. Following experimentation, electrode positions were confirmed histologically and those clearly falling outside of binocular V1 layer 4 were excluded from analysis (described below). All recordings were performed blind to group assignment.

Visually-evoked behavior in head-fixed mice.: In the head-fixed mice described above, behavioral data was obtained in parallel to all electrophysiological recordings. Although visual sequences typically elicit spontaneous behavioral responses when initially presented to naïve mice, this rapidly habituates in a manner that lacks sequence-specificity (*unpublished observations*). Thus vidget behavior was analyzed only during the SRP protocol. Mice were positioned with their forepaws on a modified piezoelectric pressure sensor (C.B. Gitty, #50-004-02) affixed directly beneath the head restraint bar, with the edge of the sensor resting inside the tube containing the animal's torso (see Figure 1D). The continuous analog signal was amplified, digitized, and recorded concurrently with the electrophysiological data using the Plexon Recorder-64 system. To quantify visually-evoked fidgeting ("vidget") behaviors, the 1000 Hz voltage recordings were downsampled to 100 Hz, and rectified (by subtracting mean voltage), and converteding to absolute values. To obtain the average vidget response to the onset of each block of grating stimuli, the 5-sec of data collected immediately after onset (typically the first 10 phase reversals) were normalized to the mean activity of the preceding 10-sec of gray screen exposure. These normalized 5-sec intervals were then averaged across blocks and the mean value was computed to generate a vidget magnitude for each stimulus in a recording session (in arbitrary units; a.u.). To quantify spontaneous behavioral movement during gray screen (Figure S1C) we simply averaged all 10-sec pre-stimulus intervals within a session for each mouse.

Object displacement task.: After completion of electrophysiological recordings, mice used in the SRP experiments were subjected to an object displacement task as a positive behavioral control to functionally confirm hippocampal ablation[28,29]. Mice were transported daily to a dimly lit room and permitted to acclimate for at least one hour prior to experimentation. Mice were then placed into a square open-field arena (40 × 40 × 30 cm) with clear plexiglass sides, located in the center of a large isolation chamber (as described above). Computer monitors were positioned on two opposing sides of the arena, each displaying full-field isoluminant gray static stimuli to provide ambient lighting. Solid white two-dimensional geometric shapes were affixed to the black walls of the isolation chamber to serve as distal spatial cues that were each visible from any location within the arena. The first day of the task consisted of two 15-minute habituation sessions to an empty arena. On each of the next two days each mouse was returned to the arena for two

10-minute sampling sessions, during which the animal could freely explore two identical objects (small glass bottles filled with odorless colored liquid) positioned in opposite corners of the arena (approximately 5 cm away from the nearest walls). The position of the objects remained consistent across days, but varied across mice. Approximately 4–6 hours separated the sampling sessions each day. Approximately 24±1 hours from the final sampling session, the mice were returned to the arena, at which time one of the two objects had been shifted to a new corner.

Exploration was manually scored by an experimenter blind to treatment condition and object identity (i.e. familiar or novel position). Exploration was quantified as the duration of time the mouse spent actively investigating each object (nose of mouse within 2 cm and facing towards the item while actively whisking). An *exploration ratio* was calculated by subtracting the time spent investigating the stimulus in the familiar position from the time spent investigating the displaced object (novel location), divided by total object exploration time. As mice rapidly habituate to new objects and their spatial positions, only the first 2 minutes of exploration was analyzed for each session.

Post-mortem histology.: To histologically quantify the extent of hippocampal lesioning, all mice were deeply anesthetized using Fatal-Plus (pentobarbital) and received 10-second bouts of direct current stimulation (2.0 mA) to each V1 electrode to better delineate the implantation depth (WPI Stimulus Isolator, model A360). Several minutes later they were slowly perfused transcardially with 0.01M phosphate-buffered saline (PBS) followed by cold 4% paraformaldehyde (PFA). Brains remained in 4% PFA at 4°C for 24 hours before being transferred to PBS for storage. Fixed brains were sliced into 50 um sections using a vibratome and briefly stored in PBS-filled wellplates at 4°C. Every sixth slice (~300 μm increments) was then processed for NeuN neuronal nuclei immunohistochemistry to aid in visualizing hippocampal ablation[77].

For the immunohistochemistry procedure, multi-well plates containing floating slices were placed on a rotary shaker and incubated in blocking solution (20% fetal bovine serum, 0.2% Triton X-100 in 0.01M PBS) for 1 hour at room temperature. Following thorough aspiration of the blocking solution, slices were incubated overnight at 4°C in mouse anti-NeuN primary antibody (#MAB377, RRID:AB_2298772, Millipore Sigma, Billerica, MA) at a 1:1000 concentration in diluted blocking solution (10% fetal plus, 0.1% Triton X-100 in 0.01M PBS). After removing primary antibody, slices were washed 3 times in PBS and incubated for a further hour at room temperature in diluted blocking solution containing 1:500 goat anti-mouse Alexa488-conjugated IgG secondary antibody (#A28175, RRID:AB_2536161, Invitrogen, Carlsbad, CA) and 1:5000 Hoechst stain (Thermo Scientific, #33342). After three additional washes slices were mounted on charged glass slides (Superfront Plus, Fisher Scientific), briefly air-dried, then coverslipped with #1.5 glass using Prolong Diamond antifade mountant (Molecular Probes, #P36961). Slices were imaged with 2x and/or 4x objective lenses on a confocal fluorescence microscope (Olympus, Japan) and tile stitching was performed using the FIJI distribution of ImageJ software[78] (NIH; RRID:SCR_002285). Lesion volumes were estimated by measuring the area of residual hippocampal tissue bilaterally across multiple coronal sections, calculated as a percentage of hippocampal tissue for the sham control group.

For post-mortem histological verification of electrode placements (in non-lesioned cohorts), mice were deeply anesthetized via isoflurane inhalation and decapitated. The brain was carefully extracted and placed in 4% PFA for 48–72 hours at 4°C, then rinsed and transferred to 0.01M PBS for storage. Brain slices (50 um) were collected using a vibratome and mounted on charged glass slides, air-dried for approximately 24 hours, then processed using cresyl violet Nissl stain. Slides were later coverslipped (#1.5 glass) with Permount mounting medium (Fisher Chemical, SP15). A confocal microscope was used to visualize Nissl staining using the bright-field channel.

Assessment of electrode tract position and accompanying tissue damage within V1 and hippocampus was assessed with reference to a mouse brain atlas[79].

QUANTIFICATION AND STATISTICAL ANALYSIS

Throughout the results section, all data is expressed as group mean ± standard error of the mean (S.E.M.). Each dataset was assessed for normality and homogeneity of variance prior to choosing a statistical approach, using Levene's, D'Agostino and Pearson, and, in the case of small sample sizes, Shapiro-Wilk tests. Two-way repeated-measures (RM) analysis-of-variance (ANOVA) were used to compare group responses across trials, blocks, days, or stimulus orientations. Greenhouse-Geisser was used to modify the degrees of freedom of repeated measures tests to correct for violations of sphericity. Interactions were followed by tests of simple main effects. Comparisons of individual values between groups (i.e. Day-1 VEP magnitudes or F/N ratios) were tested with unpaired, two-tailed t-tests. In some instances, differences between group means and baseline scores or F/N ratio parity were evaluated using one-sample *t*-tests. When datasets did not meet the assumptions required for two-way repeated-measures ANOVA, non-parametric methods were applied independently for each group (Friedman or paired Wilcoxon signed-rank tests). When appropriate, groups were then compared using ratios of responses to familiar and novel stimuli (Mann-Whitney *U* test, exact *p*-values reported). Welch's method was used to adjust *t*-tests for which normally distributed data had unequal variance. Contingent on the specific statistical test, Sidak's, Dunnett's, Dunn's, or Bonferroni methods were applied to compensate for multiple comparisons. Multiple linear regression models were used to dissociate the unique contribution of experimental group assignment to experience-dependent response changes across mice, adjusting for Day 1 (baseline) VEP magnitudes. Uncorrected alpha was set to 0.05. Statistical analyses were performed with Prism 8 (GraphPad; RRID:SCR_002798) and SPSS 25.0 (IBM; RRID:SCR_002865). Sample sizes (*n*) represents the number of animals, reported within the relevant figure caption, or alongside statistical analyses when described only in the Results.

Exclusion criteria.—Animals were excluded on the basis of a number of predefined criteria. First, experimentation was discontinued in those exhibiting evidence of illness or distress, post-operative infection, eye damage, or behavioral abnormalities (i.e. excessive grooming, discoordination, etc). Within the first days of post-operative recovery behavioral abnormalities were observed in a minority of mice that received hippocampal lesions, attributable in most cases to sub-optimal equipment performance (i.e. blocked/leaking infusion pipette). Mice were also immediately euthanized in the rare case of detachment

of the electrode headcap. Mice were excluded from analysis if electrode placement was located discernably outside of binocular V1 layer-4, as identified electrophysiologically and histologically. Specifically, mice were excluded if mean VEP morphology was abnormal or magnitude during any session fell within 2 standard deviations of baseline "noise" (spontaneous potentials measured during gray screen) in the hemisphere selected for analysis (Figure 1: sham, n = 1; lesion, n = 1; Figure 3: n = 1 [lesion group]). Predefined exclusion criteria for NMDA lesions also included: 1) insufficient hippocampal ablation (>90% residual tissue); or 2) gross extrahippocampal damage in LGN and/or visual thalamic nuclei. In practice no mice were excluded from any experiment reported within this study based on insufficient hippocampal damage, which was only encountered during pilot testing. Mice with discernable damage to visual thalamus or V1 were excluded (Figure 1–2: lesion, n = 1), except where limited atrophy was directly attributable to the LFP electrodes in V1. Spatially-restricted damage to regions immediately adjacent to the infusion pipette tracts was often evident, but did not impinge on V1. In practice, more extensive extrahippocampal tissue damage caused by NMDA was often accompanied by behavioral abnormalities and associated with poor post-operative recovery (n = 1 lesion subjects excluded from Figure 1–2, and $n = 2$ lesion subjects from Figure 3). Exclusions were performed blind to group assignment, with the exception that each cage was required to contained at least one mouse from each experimental group. Although we did not use a paired design, if all cagemates from one experimental group did not meet inclusion criteria then the littermates were also excluded ($n = 1$ sham control removed from Figs 1–2, and $n = 2$ sham controls excluded from Figure 3). Finally, a subset of mice was excluded from the cohort that received a second SRP test on Day 17 (Figure S1E–G). A littermate pair ($n = 1$/group) was excluded due to declining LFP quality, and a further 2 mice/group were used to pilot a distinct protocol (*not reported*) and could not be retested.

Supplementary Material

Refer to Web version on PubMed Central for supplementary material.

Acknowledgements.

We are very grateful to Arnold Heynen, Suzanne Meagher, Nina Palisano, Jessica Buckey, Erik Sklar, Kiki Chu, Amanda Coronado, Athene Wilson-Glover, Katherine Marshall, and Erin Hickey for their administrative and technical support. We particularly thank Alyssa (Ying) Li for assistance during pilot experiments, behavioral scoring, immunohistochemistry, and confocal histology, as well as Julie (Heejung) Kim, who contributed to histology. We gratefully acknowledge Jeff Gavornik and Dustin Hayden for developing software used in the collection and analysis of this data. Christian Candler assisted in replicating reported datasets. Thanks also to Sam Cooke and Ming-fai Fong for their scientific insights, and to Lara Pierce for guidance on statistical methodologies. This work was supported by the National Institutes of Health (R01EY023037; MFB), the Picower Institute Innovation Fund (MFB), and the JPB Foundation Picower Fellows program (PSBF).

References

1. Squire LR (1992). Declarative and nondeclarative memory: multiple brain systems supporting learning and memory. J. Cogn. Neurosci 4, 232–243. [PubMed: 23964880]
2. Mishkin M, Suzuki WA, Gadian DG & Vargha-Khadem F (1997). Hierarchical organization of cognitive memory. Philos. Trans. R. Soc. Lond. B Biol. Sci 352, 1461–1467. [PubMed: 9368934]
3. Nissen MJ, Knopman DS & Schacter DL (1987). Neurochemical dissociation of memory systems. Neurology 37, 789–794. [PubMed: 3574678]

4. Squire LR (2004). Memory systems of the brain: a brief history and current perspective. Neurobiol. learn. and mem 82, 171–177.
5. Donato F, Alberini CM, Amso D, Dragoi G, Dranovsky A, & Newcombe NS (2021). The Ontogeny of Hippocampus-Dependent Memories. J. Neurosci 41, 920–926. [PubMed: 33328296]
6. Gavornik JP & Bear MF (2014). Higher brain functions served by the lowly rodent primary visual cortex. Learn. Mem 21, 527–533. [PubMed: 25225298]
7. Cooke SF & Bear MF (2015). Visual recognition memory: a view from V1. Curr. Opin. Neurobiol 35, 57–65. [PubMed: 26151761]
8. Frenkel MY, Sawtell NB, Diogo AC, Yoon B, Neve RL, & Beaer MF (2006). Instructive effect of visual experience in mouse visual cortex. Neuron 51, 339–349. [PubMed: 16880128]
9. Cooke SF & Bear MF (2014). How the mechanisms of long-term synaptic potentiation and depression serve experience-dependent plasticity in primary visual cortex. Philos. Trans. R. Soc. Lond. B Biol. Sci 369, 20130284. [PubMed: 24298166]
10. Aton SJ, Suresh A, Broussard C & Frank MG (2014). Sleep promotes cortical response potentiation following visual experience. Sleep 37, 1163–1170. [PubMed: 25061244]
11. Cooke SF, Komorowski RW, Kaplan ES, Gavornik JP & Bear MF (2015). Visual recognition memory, manifested as long-term habituation, requires synaptic plasticity in V1. Nat. Neurosci 18, 262–271. [PubMed: 25599221]
12. Kaplan ES, Cooke SF, Komorowski RW, Chubykin AA, Thomazeau A, Khibnik LA, Gavornik JP, & Bear MF (2016). Contrasting roles for parvalbumin-expressing inhibitory neurons in two forms of adult visual cortical plasticity. Elife 5.
13. Gavornik JP & Bear MF (2014). Learned spatiotemporal sequence recognition and prediction in primary visual cortex. Nat. Neurosci 17, 732–737. [PubMed: 24657967]
14. Barron HC, Auksztulewicz R & Friston K (2020). Prediction and memory: A predictive coding account. Prog. in neurobiol 192, 101821.
15. Muhammad R (2009). The mouse visually evoked potential: neural correlates and functional applications Ph.D. thesis, Massachusetts Institute of Technology.
16. Devito LM & Eichenbaum H (2011). Memory for the order of events in specific sequences: contributions of the hippocampus and medial prefrontal cortex. J. Neurosci 31, 3169–3175. [PubMed: 21368028]
17. van den Broek SP, Reinders F, Donderwinkel M & Peters MJ (1998). Volume conduction effects in EEG and MEG. Electroencephalogr. Clin. Neurophysiol 106, 522–534. [PubMed: 9741752]
18. O'Neill PK, Gordon JA & Sigurdsson T (2013). Theta oscillations in the medial prefrontal cortex are modulated by spatial working memory and synchronize with the hippocampus through its ventral subregion. J. Neurosci 33, 14211–14224. [PubMed: 23986255]
19. Diekelmann S & Born J (2010). The memory function of sleep. Nat. Rev. Neurosci 11, 114–126. [PubMed: 20046194]
20. Parish G, Hanslmayr S & Bowman H (2018). The Sync/deSync Model: How a Synchronized Hippocampus and a Desynchronized Neocortex Code Memories. J. Neurosci 38, 3428–3440. [PubMed: 29487122]
21. Siapas AG, Lubenov EV & Wilson MA (2005). Prefrontal phase locking to hippocampal theta oscillations. Neuron 46, 141–151. [PubMed: 15820700]
22. Sirota A Montgomery S, Fujisawa S, Isomura Y, Zugaro M, & Buzsaki G (2008). Entrainment of neocortical neurons and gamma oscillations by the hippocampal theta rhythm. Neuron 60, 683–697. [PubMed: 19038224]
23. Carrera E & Tononi G (2014). Diaschisis: past, present, future. Brain 137, 2408–2422. [PubMed: 24871646]
24. Stone ME, Grimes BS & Katz DB (2005). Hippocampal inactivation enhances taste learning. Learn. Mem 12, 579–586. [PubMed: 16322360]
25. Schroeder JP, Wingard JC & Packard MG (2002). Post-training reversible inactivation of hippocampus reveals interference between memory systems. Hippocampus 12, 280–284. [PubMed: 12000124]

26. Oliveira AM, Hawk JD, Abel T & Havekes R (2010). Post-training reversible inactivation of the hippocampus enhances novel object recognition memory. Learn. Mem 17, 155–160. [PubMed: 20189960]
27. Sawangjit A, Oyanedel CN, Niethard N, Salazar C, Born J, & Inostroza M (2018). The hippocampus is crucial for forming non-hippocampal long-term memory during sleep. Nature 564, 109–113. [PubMed: 30429612]
28. Murai T, Okuda S, Tanaka T & Ohta H (2007). Characteristics of object location memory in mice: Behavioral and pharmacological studies. Physiol. & Behav 90, 116–124. [PubMed: 17049363]
29. Barker GR & Warburton EC Evaluating the neural basis of temporal order memory for visual stimuli in the rat. Eur. J. Neurosci 33, 705–716. [PubMed: 21226775]
30. Barker GR & Warburton EC (2015). Object-in-place associative recognition memory depends on glutamate receptor neurotransmission within two defined hippocampal-cortical circuits: a critical role for AMPA and NMDA receptors in the hippocampus, perirhinal, and prefrontal cortices. Cereb. Cortex 25, 472–481. [PubMed: 24035904]
31. Konkel A, Warren DE, Duff MC, Tranel DN & Cohen NJ (2008). Hippocampal amnesia impairs all manner of relational memory. Front. Hum. Neurosci 2, 15. [PubMed: 18989388]
32. Barker GRI & Warburton EC (2010). Putting objects in context: A prefrontal-hippocampal-perirhinal cortex network. Brain Neurosci. Adv 4, 2398212820937621.
33. Konkel A & Cohen NJ (2009). Relational memory and the hippocampus: representations and methods. Front. Neurosci 3, 166–174. [PubMed: 20011138]
34. Rolls ET (2013). The mechanisms for pattern completion and pattern separation in the hippocampus. Front. Syst. Neurosci 7, 74. [PubMed: 24198767]
35. Eichenbaum H & Fortin NJ (2009). The neurobiology of memory based predictions. Philos. Trans. R. Soc. Lond. B Biol. Sci 364, 1183–1191. [PubMed: 19527999]
36. Xu S, Jiang W, Poo MM & Dan Y (2012). Activity recall in a visual cortical ensemble. Nat. Neurosci 15, 449–455. [PubMed: 22267160]
37. Kim T, Chaloner FA, Cooke SF, Harnett MT & Bear MF (2019). Opposing Somatic and Dendritic Expression of Stimulus-Selective Response Plasticity in Mouse Primary Visual Cortex. Front. Cell. Neurosci 13, 555. [PubMed: 32009901]
38. Hayden DJ, Montgomery DP, Cooke SF & Bear MF Visual recognition is heralded by shifts in local field potential oscillations and inhibitory networks in primary visual cortex. (2021). J. Neurosci, JN-RM-0391–21.
39. Papanikolaou A Rodrigues FR, Holeniewska J, Phillips K, Saleem AB, & Solomon SG (2020). Plasticity in visual cortex is disrupted in a mouse model of tauopathy and neurodegeneration. bioRxiv, 2020.2011.2002.365767.
40. Cooke SF & Bear MF (2010). Visual experience induces long-term potentiation in the primary visual cortex. J. Neurosci 30, 16304–16313. [PubMed: 21123576]
41. Whittington JCR Muller TH, Mark S, Chen G, Barry C, Burgess N, & Behrens TEJ (2020). The Tolman-Eichenbaum Machine: Unifying Space and Relational Memory through Generalization in the Hippocampal Formation. Cell 183, 1249–1263. [PubMed: 33181068]
42. Clayton NS, Bussey TJ & Dickinson A (2003). Can animals recall the past and plan for the future? Nat. Rev. Neurosci 4, 685–691. [PubMed: 12894243]
43. Warburton EC & Brown MW (2015). Neural circuitry for rat recognition memory. Behav. Brain Res 285, 131–139. [PubMed: 25315129]
44. Kesner RP, Gilbert PE & Barua LA (2002). The role of the hippocampus in memory for the temporal order of a sequence of odors. Behav. Neurosci 116, 286–290. [PubMed: 11996313]
45. Fortin NJ, Agster KL & Eichenbaum HB (2002). Critical role of the hippocampus in memory for sequences of events. Nat. Neurosci 5, 458–462. [PubMed: 11976705]
46. Teyler TJ & DiScenna P (1986). The hippocampal memory indexing theory. Behav. Neurosci 100, 147–154. [PubMed: 3008780]
47. Marr D (1971). Simple memory: a theory for archicortex. Philos. Trans. R. Soc. Lond. B Biol. Sci 262, 23–81. [PubMed: 4399412]

48. Cheng S (2013). The CRISP theory of hippocampal function in episodic memory. Front. Neur. Circuits 7, 88.
49. Fiser A, Mahringer D, Oyibo HK, Petersen AV, Leinweber M, & Keller GB (2016). Experience-dependent spatial expectations in mouse visual cortex. Nat. Neurosci 19, 1658–1664. [PubMed: 27618309]
50. Esteves IM, Chang H, Neumann AR, Sun J, Mohajerani MH, & McNaughton BL (2021). Spatial Information Encoding across Multiple Neocortical Regions Depends on an Intact Hippocampus. J. Neurosci 41, 307–319. [PubMed: 33203745]
51. Gershman SJ (2017). Predicting the Past, Remembering the Future. Curr. Opin. Behav. Sci 17, 7–13. [PubMed: 28920071]
52. Bastos AM, Usrey WM, Adams RA, Mangun GR, Fries P, & Friston KJ (2012). Canonical microcircuits for predictive coding. Neuron 76, 695–711. [PubMed: 23177956]
53. Keller GB & Mrsic-Flogel TD (2018). Predictive Processing: A Canonical Cortical Computation. Neuron 100.
54. Rajasethupathy P, Sankaran S, Marshel JH, Kim CK, Ferenczi E, Lee SY, Berndt A, Ramakrishnan C, Jaffe A, Lo M, et al. (2015). Projections from neocortex mediate top-down control of memory retrieval. Nature 526, 653–659. [PubMed: 26436451]
55. Zhang S, Xu M, Kamigaki T, Hoang Do JP, Chang WC, Jenvay S, Miyamichi K, Luo L, & Dan Y (2014). Selective attention. Long-range and local circuits for top-down modulation of visual cortex processing. Science 345, 660–665. [PubMed: 25104383]
56. Morimoto MM, Uchishiba E & Saleem AB (2021). Organization of feedback projections to mouse primary visual cortex. iScience, 102450.
57. Sidorov MS, Kim H, Rougie M, Williams B, Siegel JJ, Gavornik JP, & Philpot BD (2020). Visual Sequences Drive Experience-Dependent Plasticity in Mouse Anterior Cingulate Cortex. Cell. Rep 32, 108152. [PubMed: 32937128]
58. Takacs VT, Freund TF & Gulyas AI (2008). Types and synaptic connections of hippocampal inhibitory neurons reciprocally connected with the medial septum. Eur. J. Neurosci 28, 148–164. [PubMed: 18662340]
59. Mattis J, Brill J, Evans S, Lerner TN, Davidson TJ, Hyun M, Ramakrishnan C, Deisseroth K, & Huguenard JR (2014). Frequency-dependent, cell type-divergent signaling in the hippocamposeptal projection. J. Neurosci 34, 11769–11780. [PubMed: 25164672]
60. Dragoi G, Carpi D, Recce M, Csicsvari J & Buzsaki G (1999). Interactions between hippocampus and medial septum during sharp waves and theta oscillation in the behaving rat. J. Neurosci 19, 6191–6199. [PubMed: 10407055]
61. Lean GA, Liu YJ & Lyon DC (2019). Cell type specific tracing of the subcortical input to primary visual cortex from the basal forebrain. J. Comp. Neurol 527, 589–599. [PubMed: 29441578]
62. Goard M & Dan Y (2009). Basal forebrain activation enhances cortical coding of natural scenes. Nat. Neurosci 12, 1444–1449. [PubMed: 19801988]
63. Pinto L, Goard MJ, Estandian D, Xu M, Kwan AC, Lee SH, Harrison TC, Feng G, & Dan Y (2013). Fast modulation of visual perception by basal forebrain cholinergic neurons. Nat. Neurosci 16, 1857–1863. [PubMed: 24162654]
64. Minces V, Pinto L, Dan Y & Chiba AA (2017). Cholinergic shaping of neural correlations. PNAS 114, 5725–5730. [PubMed: 28507133]
65. Chubykin AA, Roach EB, Bear MF & Shuler MG (2013). A cholinergic mechanism for reward timing within primary visual cortex. Neuron 77, 723–735. [PubMed: 23439124]
66. Cone I & Shouval HZ (2021). Learning precise spatiotemporal sequences via biophysically realistic learning rules in a modular, spiking network. Elife 10.
67. Krueger JN, Wilmot JH, Teratani-Ota Y, Puhger KR, Nemes SE, Crestani AP, Lafreniere MM, & Wiltgen BJ (2020). Amnesia for context fear is caused by widespread disruption of hippocampal activity. Neurobiol. Learn. Mem 175, 107295. [PubMed: 32822864]
68. Otchy TM Wolff SB, Rhee JY, Pehlevan C, Kawai R, Kempf A, Gobes SM, & Olveczky BP (2015). Acute off-target effects of neural circuit manipulations. Nature 528, 358–363. [PubMed: 26649821]

69. O'Reilly RC, Bhattacharyya R, Howard MD & Ketz N (2014). Complementary learning systems. Cogn. Sci 38, 1229–1248. [PubMed: 22141588]

70. McClelland JL, McNaughton BL & O'Reilly RC (1995). Why there are complementary learning systems in the hippocampus and neocortex: insights from the successes and failures of connectionist models of learning and memory. Psychol. Rev 102, 419–457. [PubMed: 7624455]

71. Racine RJ, Chapman CA, Trepel C, Teskey GC & Milgram NW (1995). Post-activation potentiation in the neocortex. IV. Multiple sessions required for induction of long-term potentiation in the chronic preparation. Brain Res. 702, 87–93. [PubMed: 8846100]

72. Buzsaki G (1989). Two-stage model of memory trace formation: a role for "noisy" brain states. Neuroscience 31, 551–570. [PubMed: 2687720]

73. Ji D & Wilson MA (2007). Coordinated memory replay in the visual cortex and hippocampus during sleep. Nat. Neurosci 10, 100–107. [PubMed: 17173043]

74. Girardeau G, Benchenane K, Wiener SI, Buzsaki G & Zugaro MB (2009). Selective suppression of hippocampal ripples impairs spatial memory. Nat. Neurosci 12, 1222–1223. [PubMed: 19749750]

75. Peyrache A & Seibt J (2020). A mechanism for learning with sleep spindles. Philos. Trans. R. Soc. Lond. B Biol. Sci 375, 20190230. [PubMed: 32248788]

76. Howard MW, Fotedar MS, Datey AV & Hasselmo ME (2005). The temporal context model in spatial navigation and relational learning: toward a common explanation of medial temporal lobe function across domains. Psychol. Rev 112, 75–116. [PubMed: 15631589]

77. Wang SH, Teixeira CM, Wheeler AL & Frankland PW (2009). The precision of remote context memories does not require the hippocampus. Nat. Neurosci 12, 253–255. [PubMed: 19182794]

78. Schindelin J, Schindelin J, Arganda-Carreras I, Frise E, Kaynig V, Longair M, Pietzsch T, Preibisch S, Rueden C, Saalfeld S, & Schmid B (2012). Fiji: an open-source platform for biological-image analysis. Nat. Methods 9, 676–682. [PubMed: 22743772]

79. Franklin KB & Paxinos G (2008). The mouse brain in stereotaxic coordinates.

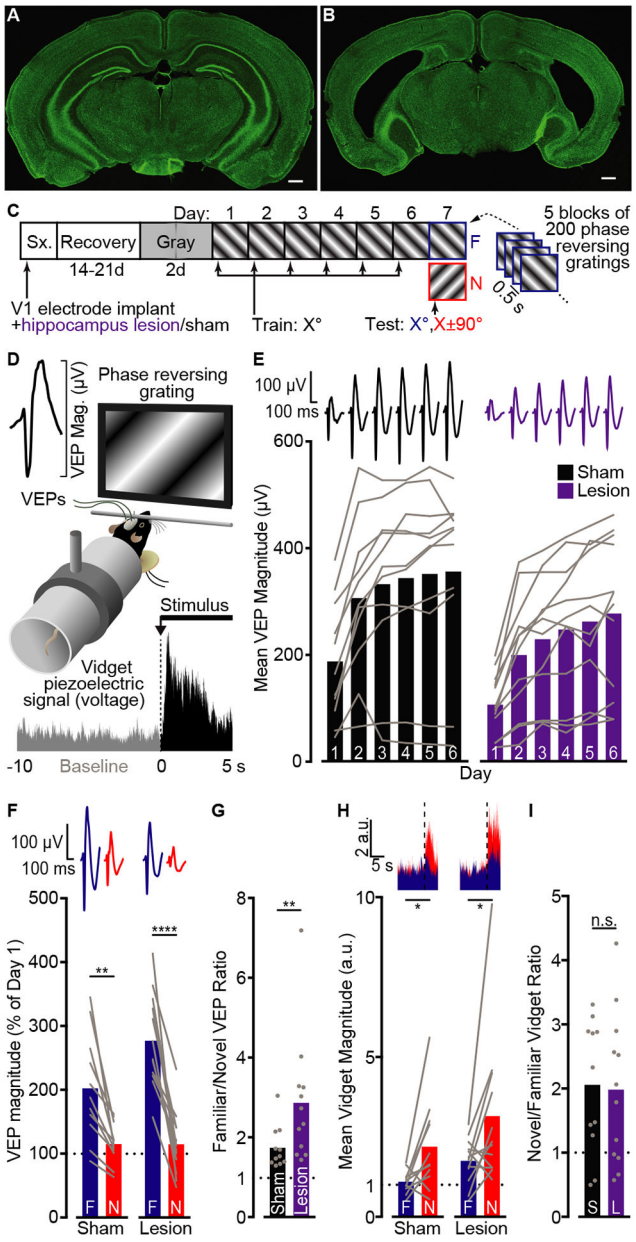

Figure 1. Long-term visual recognition memory does not require the hippocampus.

Representative coronal brain sections processed via NeuN immunofluorescence from mice in (**A**) sham control and (**B**) hippocampal lesion groups. The mouse depicted in the lesion example retained 40.77% residual hippocampal tissue across all quantified coronal sections, relative to the mean area of the sham control group. Green, NeuN. Scale bar represents 500 μm. Diagrams depict the **(C)** experimental protocol and **(D)** apparatus. **(E)** Mean VEP magnitudes plotted for each training day (days inset along x-axis, mean daily voltage traces plotted at top, and lines depict mean magnitude for each mouse). In both groups VEPs potentiated across days of exposure to a grating stimulus (two-way repeated-measures [RM] ANOVA with Greenhouse-Geisser correction, effect of day [$F_{1.859,39.04} = 50.96$, $p < 0.0001$]; Sidak's posthoc tests comparing Days 1 to 2–6, each $p < 0.0001$). However,

potentiation did not differ between Sham (S) and Lesion (L) groups (neither a main effect of group [$F_{1,21}$ = 2.89, p = 0.1] nor group by day interaction [$F_{1.859,39.04}$ = 0.44, p = 0.63]). **F)** VEP magnitudes elicited by familiar (F) and novel (N) stimulus orientations on *Day 7*, normalized to *Day 1*. The difference in familiar versus novel responses was significantly larger in the Lesion relative to Sham group (RM ANOVA group by stimulus interaction; $F_{1,21}$ = 6.03, p = 0.023; Sidak's post hoc tests: F vs N, Sham p = 0.0017, Lesion p < 0.0001). **G)** The ratio of VEP magnitudes elicited by F relative to N was also larger in the Lesion versus Sham group (two-tailed Mann-Whitney U = 24, n_{sham} = 11, n_{lesion} = 12, p = 0.009), confirming that SRP is exaggerated following hippocampal ablation. **H)** In each group, larger mean behavioral response magnitudes (arbitrary units, a.u.) were elicited by the onset of N versus F stimuli on Day 7 (mean traces superimposed at top; two-tailed Wilcoxon matched-pairs planned comparisons: sham, Z = 2.223, p = 0.024; lesion, Z = 2.118, p = 0.034). **I)** The Novel/Familiar vidget ratios for each group were comparable (unpaired two-tailed t-test, t_{21} = 0.16, p = 0.88). *p < 0.05, **p <0.01, *** p < 0.001, ****p < 0.0001, not significant (n.s.) p > 0.05. n/group: Sham = 11, Lesion = 12. See also Figures S1–S2; Table S1.

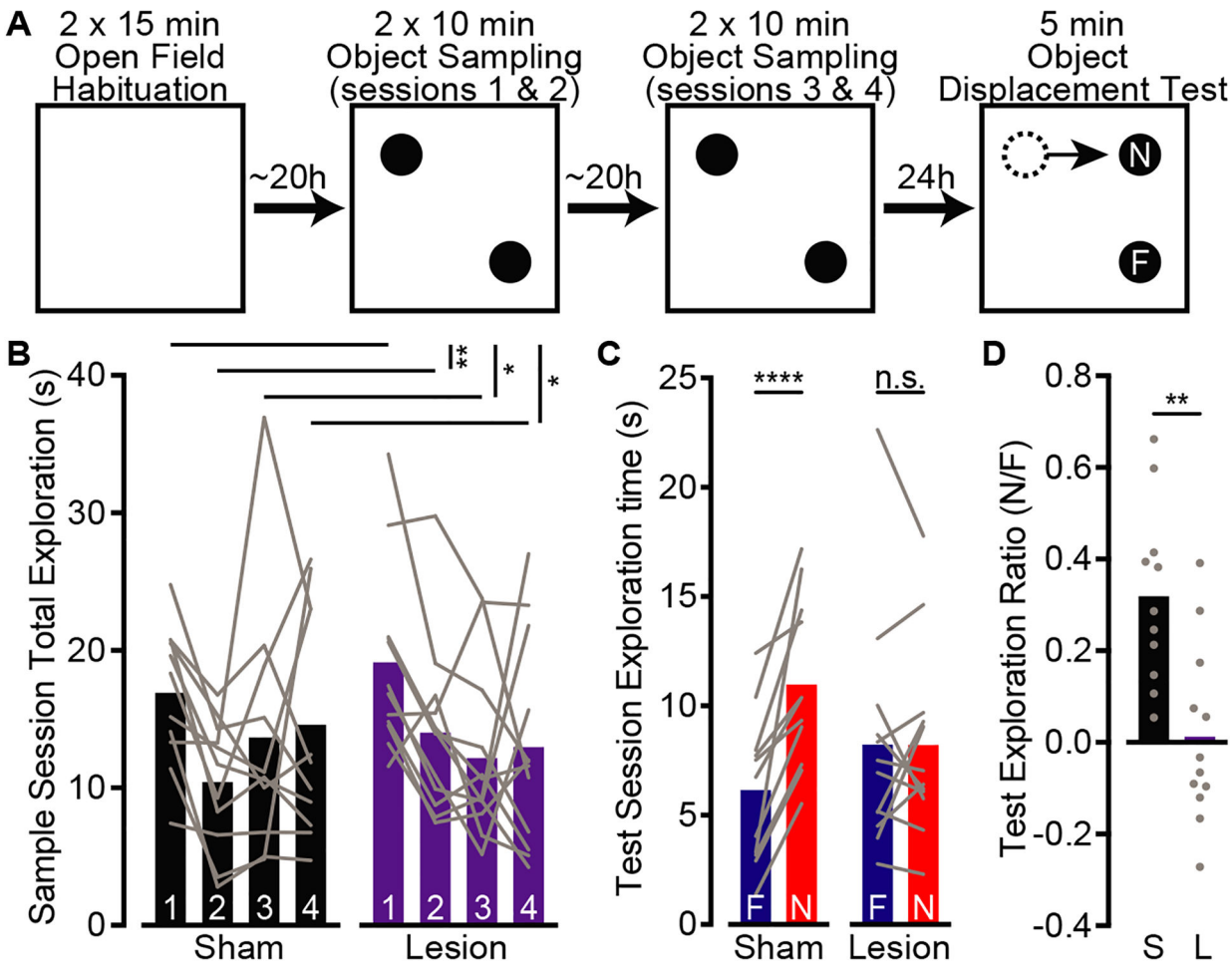

Figure 2. Pre-training hippocampal lesions impair spontaneous exploration of a spatially-displaced object.

A) Diagram of experimental timeline and apparatus. Square boxes represent overhead views of the open field arena, and filled circles example positions of identical objects during sampling and testing phases. **B)** The average time mice explored two identical objects declined between the first and each subsequent sampling sessions (two-way RM ANOVA with Greenhouse-Geisser correction, main effect of session, $F_{2.071,43.482} = 4.38$, $p = 0.017$; Dunnetts's posthoc tests comparing Sessions 1 with 2 ($p = 0.005$), 3 (p = 0.013), and 4 (p = 0.049)). There was no difference in exploration between Lesion and Sham groups during the sampling sessions (main effect of Group, $F_{1,21} = 0.13$, $p = 0.73$; Group by Session interaction, $F_{2.071,43.482} = 1.13$, $p = 0.34$). **C)** On test day the Sham group explored a spatially displaced object for a significantly longer duration (N mean = 10.97±1.17 s) than a static object (F mean = 6.15±1.04 sec; treatment by object interaction: $F_{1,21} = 14.03$, $p = 0.001$; Sidak's multiple comparison test, $p < 0.0001$), whereas the lesion group explored both objects equivalently (F = 8.23±1.55 sec; N = 8.21±1.25 s; Sidak's, $p > 0.99$). **D)** A ratio of exploration times for the N versus F object was also significantly greater for the Sham (0.31 ± 0.05 a.u.) relative to Lesion (0.012 ± 0.06 a.u.) group (two-tailed unpaired $t_{21} = 3.79$, $p = 0.001$). * < 0.05, ** < 0.01, **** < 0.0001. *n*/group: Sham = 11, Lesion = 12. See also Table S1.

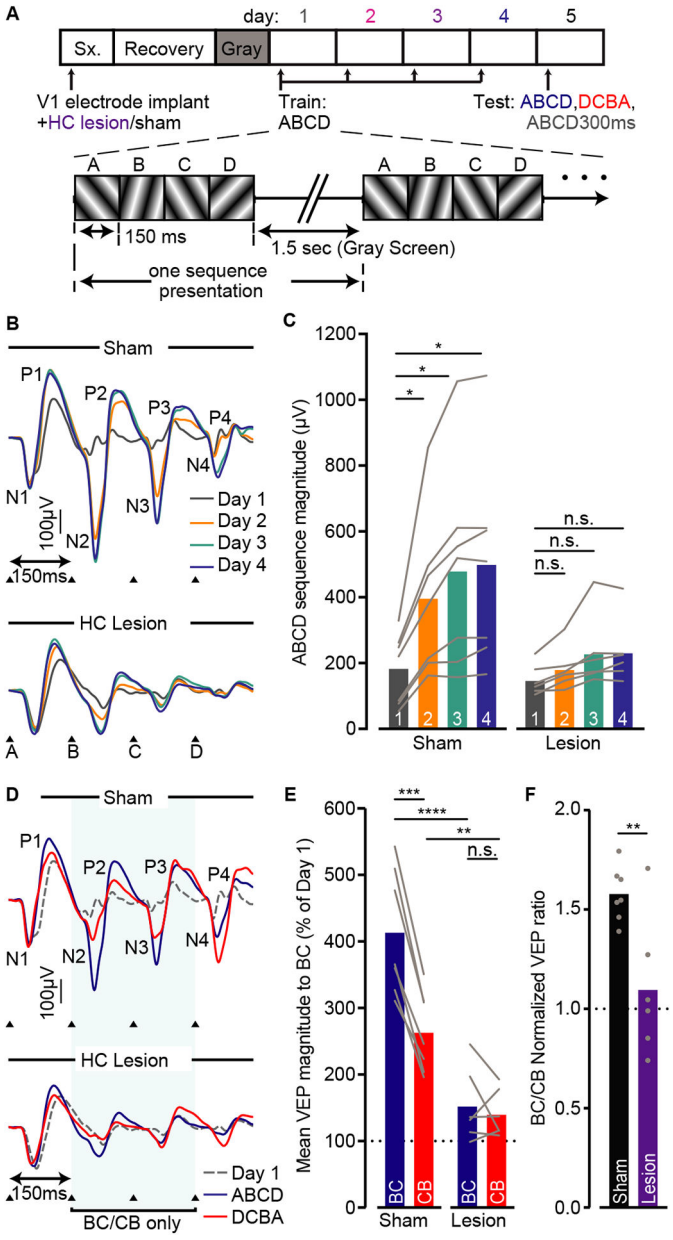

Figure 3. The hippocampus is required for V1 response potentiation evoked by a sequence of visual stimuli.

A) Schematic diagram of experimental time-course and daily visual stimulation protocol. **B)** Average VEP waveforms elicited by visual sequence *ABCD* for each group on *days 1–4*. Labeled arrows denote the onset latency of sequence elements A, B, C, and D. N1–4 and P1–4 labels refer, respectively, to the four peak negative- and positive-going deflections of the V1 local field potential following each stimulus onset. **C)** Potentiation of average VEP magnitude to the familiar sequence across *Days 1–4* was impaired in mice with hippocampal relative to sham lesions (two-way RM ANOVA, day by group interaction, $F_{3, 33} = 6.20$, $p = 0.0018$). Within-subject potentiation was significant for the Sham (Sidak's posthoc comparisons of *Days 1* versus *2–4*: $p = 0.024$, 0.027, and 0.022, respectively) but not Lesion group (*Day 2*, $p = 0.072$; *Day 3*, $p = 0.11$; *Day 4*, $p = 0.061$). **D)** Average VEP

waveforms elicited by sequence *ABCD* and the reverse *DCBA* during the *Day 5* test session (*Day 1* superimposed for reference). **E)** On *Day 5*, response potentiation in Lesion and Sham groups were significantly different for elements B and C in the *ABCD* versus reverse *DCBA* sequences, normalized to the *day-1* baseline magnitudes for each mouse (two-way RM ANOVA group by stimulus interaction, $F_{1, 11} = 31.73$, $p = 0.0002$). Responses to *BC* were larger in the Sham controls than in the Lesion group (planned Sidak's comparison, $p < 0.0001$), suggesting the hippocampus is required for sequence-specific potentiation. Furthermore, response magnitude to the forward (*BC*) sequence was only larger than the reverse (*CB*) in the Sham ($p < 0.0001$) but not the Lesion group ($p = 0.75$). Mean response to the reverse *CB* sequence was also significantly larger for the Sham compared to Lesion group ($p = 0.0057$), indicative of an overall difference in sequence-independent potentiation. Subsequent planned one-sample *t*-tests with Bonferroni correction revealed significant potentiation of responses to both *BC* and *CB* over the *Day-1* baseline only in the Sham ($p = 0.0004$ and 0.0016, respectively) but not the Lesion group ($p = 0.26$ and 0.15, respectively). **F)** The familiar/novel ratio on *Day 5* was also significantly larger in the Sham versus Lesion group (Welch's two-tailed *t*-test, $t_{6.316} = 3.162$, $p = 0.018$). Furthermore, planned one-sample *t*-tests confirmed that sequence-specific potentiation was only evident in the sham ($p < 0.0001$) but not lesion ($p = 0.51$) group. Bars represent group means and points/lines are mean values for each individual mouse. *$p < 0.05$, **$p < 0.01$, *** $p < 0.001$, ****$p < 0.0001$, n.s. $p > 0.05$. *n*/group: Sham = 7, Lesion = 6. See also Figure S3; Table S1.

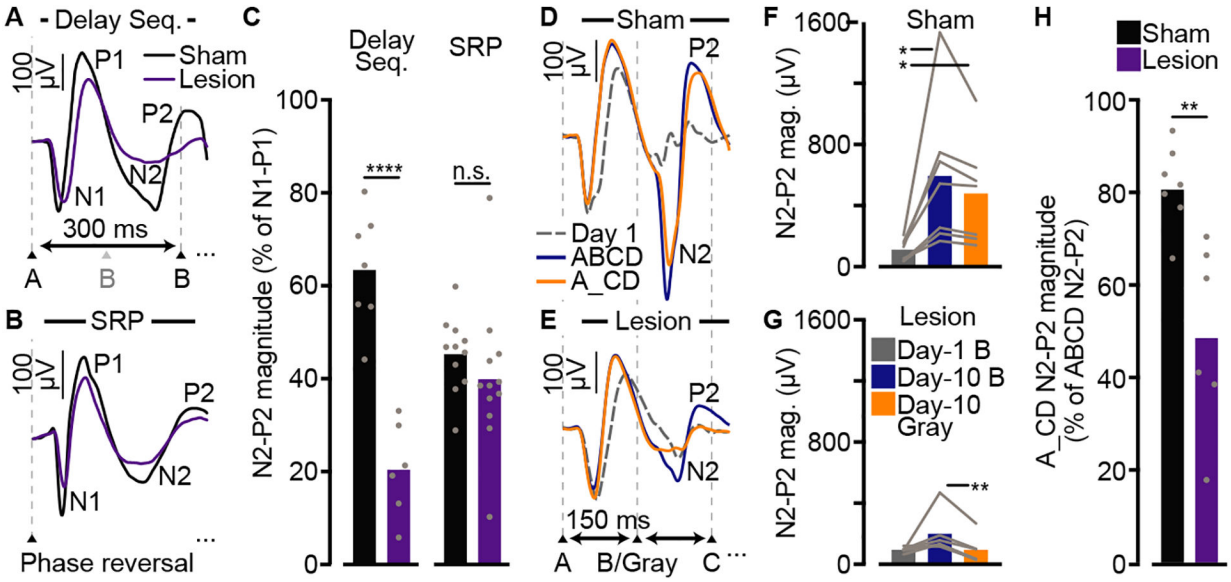

Figure 4. Hippocampal lesions impair the generation of anticipatory responses in V1.

A) In addition to presentation of the forward and reverse sequences, on Day 5 of the visual sequence protocol we included interleaved blocks of the forward ABCD sequence in which each element was displayed for twice the standard duration (300 ms instead of 150 ms). Traces depict truncated mean VEP waveforms recorded in Sham and Lesion groups following sequence onset, encompassing both early (N1, P1) and late (N2, P2) VEP components elicited by stimulus A. Hashed horizontal lines indicate the transition points between sequence elements (denoted by labeled arrows at panel bottom, with grayed 'B' indicating the standard stimulus onset time-point). **B)** Truncated mean VEP waveforms elicited in Sham and Lesion groups by the familiar grating stimulus on Day 7 of the SRP protocol (re-plotted from Figure 2). **C)** Graph displays mean N2-P2 responses elicited by stimulus A in the slowed ABCD pattern on Day 5 of the visual sequence protocol (Delay Seq.) and by the familiar grating orientation on Day 7 of the SRP protocol. To account for baseline VEP differences between groups and protocols, the trough-to-peak magnitude of the N2-P2 response was normalized to the average magnitude of P1-N1 for each mouse ([P2 – N2]/[P1 – N1] × 100). Bars represent group means, with individual data-points depicting the mean response magnitudes for each mouse. A significant group-by-protocol interaction (two-way between-groups ANOVA, $F_{1,32} = 19.31$, $p = 0.0001$) is driven by a larger P2-N2 response in sham controls than lesioned mice exposed to the visual sequence protocol (Tukey's pairwise comparison, $p < 0.0001$), but not the SRP protocol ($p = 0.51$). **D-E)** Truncated mean VEP waveforms recorded from Sham control and Lesion groups in response to the ABCD visual sequence on experimental days 1 and 10, as well as A_CD on day 10 (wherein gray screen is substituted for grating stimulus B). **F-G)** Graphs plot mean N2-P2 VEP magnitudes for the Sham and Lesion groups elicited by the 2nd element in each visual sequence (grating orientation B or gray screen). A significant group-by-sequence interaction effect (two-way RM ANOVA with Greenhouse-Geisser correction, $F_{2, 22} = 5.553$, $p = 0.011$) was driven by robust VEP potentiation in the Sham group elicited by stimulus B on Day 10 versus Day 1 (Tukey's pairwise comparisons, $p = 0.0499$) and by gray screen on Day 10 versus stimulus B on Day 1 ($p = 0.028$), but not between stimulus B and gray screen

on Day 10 ($p = 0.198$). Conversely, responses in the Lesion group to stimulus B on Day 10 are exaggerated when compared to those elicited by gray screen (Tukey's Day 10 ABCD vs A_CD comparison, $p = 0.0079$), despite a lack of response potentiation to stimulus B between Days 1 and 10 ($p = 0.244$). **H)** To directly compare generative anticipatory responses between the two groups, we analyzed the N2-P2 responses in the A_CD condition (as a percentage of the ABCD condition on Day 10). The anticipatory VEP during the omission of stimulus B was significantly larger in the Sham than the Lesion group (Welch's two-tailed t-test, $t_{7.025} = 4.552$, $p = 0.0026$). *$p < 0.05$, **$p < 0.01$, ****$p < 0.0001$, n.s. $p > 0.05$. *n*/group: Seq., Sham = 7, Lesion = 6; SRP, Sham = 11, Lesion = 12. See also Figure S3; Table S1.

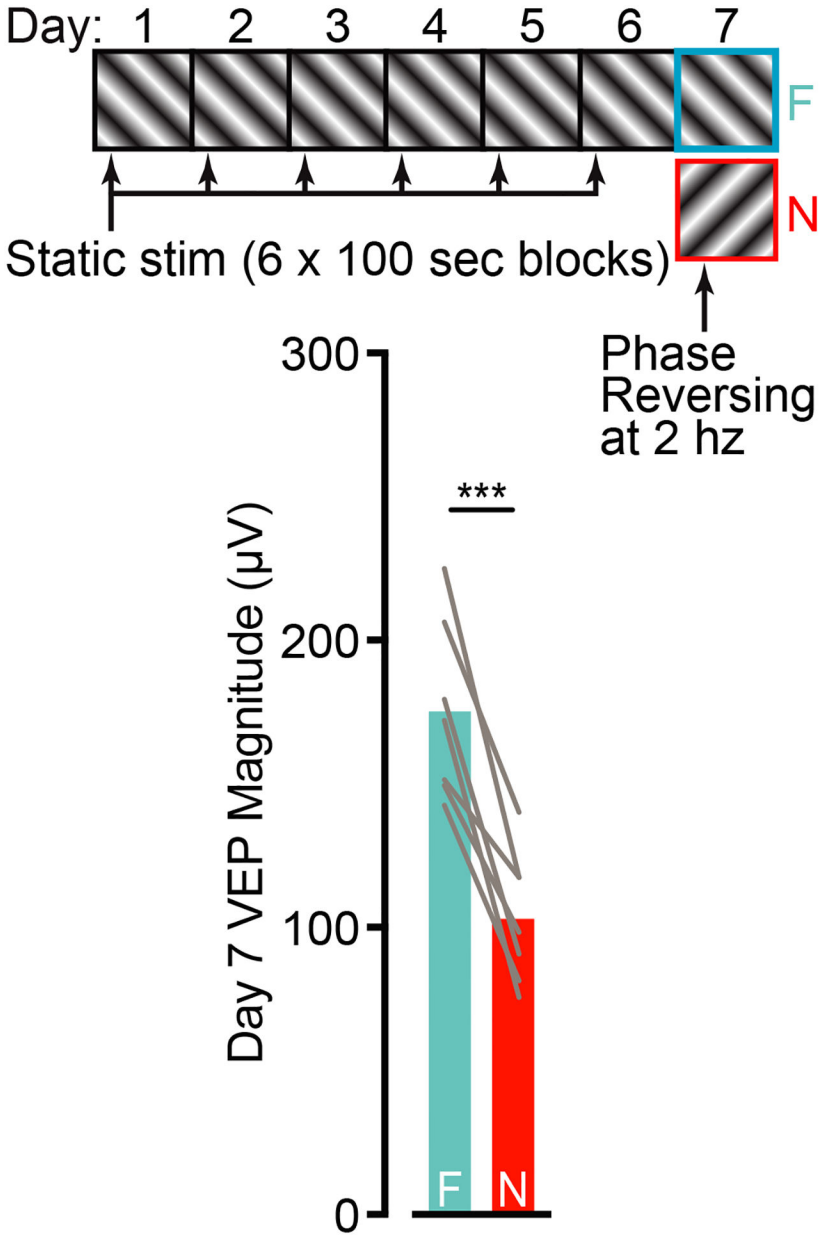

Figure 5. Daily exposure to static gratings elicits robust VEP potentiation.

Diagram summarizes a modified SRP protocol in which each mouse (N = 7) viewed 6 × 100 sec blocks of a static grating stimulus during each of 6 daily recording sessions. On the 7th day of the protocol both a familiar stimulus and a novel orientation were presented phase reversing at 2 Hz. Static stimulation elicited robust SRP, revealed by comparison to the novel orientation (paired two-tailed *t*-test, $t_6 = 7.235$, $p = 0.0004$). Thus, SRP does not require modulation of upcoming responses based on a predicted spatiotemporal pattern. ***p < 0.001.

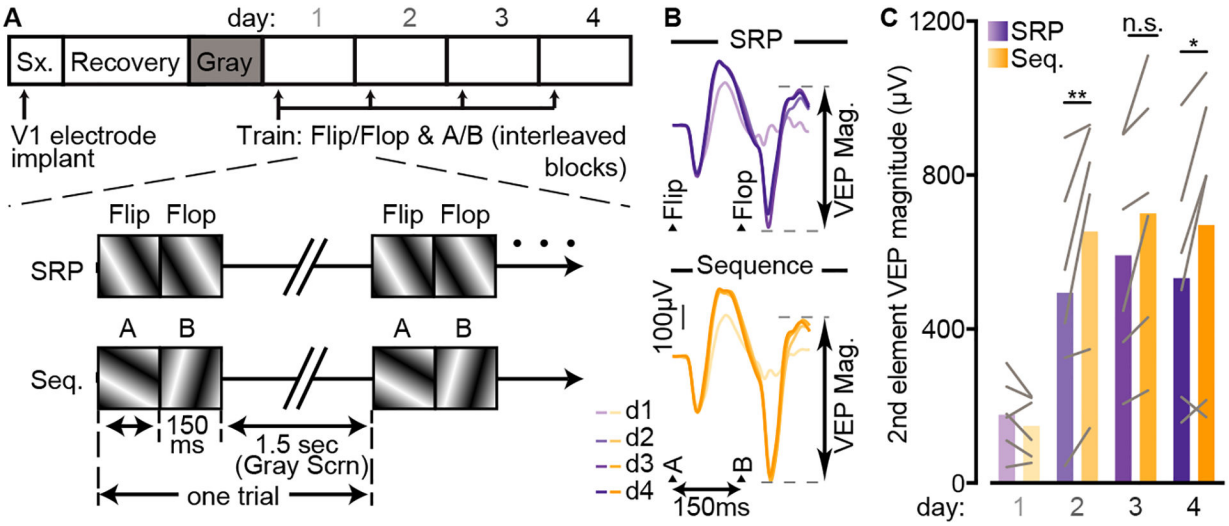

Figure 6. Orientation-shifted stimulus pairs elicit exaggerated potentiation compared to phase-shifted pairs.

A) Diagram of a modified visual stimulation protocol combining attributes of the SRP and sequence protocols. Each mouse (N = 6) views two pairs of stimuli across interleaved blocks. The pairs of stimuli are either phase- or orientation-shifted (labeled 'SRP' and 'Sequence', respectively). All other stimulation properties are identical across the two conditions. **B)** Average VEP waveforms for the SRP and sequence stimulus pairs, with ticks denoting the onset of phase reversed (flip and flop) and orientation-shifted (A and B) images. **C)** Comparing VEP magnitudes elicited by the second stimulus in each pair ('flop' vs. 'B') indicates that potentiation over days is exaggerated for the orientation-shifted compared to phase-shifted stimulus (two-way RM ANOVA, Stimulus by Day interaction, $F_{3,15} = 4.81$, $p = 0.015$; Sidak's posthoc comparisons of SRP and sequence VEPs on d1, $p = 0.92$; d2, $p = 0.0036$; d3, $p = 0.050$; d4, $p = 0.011$). We conclude that in addition to potentiation driven by familiarity with the identity of each oriented grating, during familiar visual sequences the brain predictively modulates responses to each cued stimulus, further enhancing VEP magnitude. * < 0.05, ** < 0.01, n.s. non-significant.

KEY RESOURCES TABLE

REAGENT or RESOURCE	SOURCE	IDENTIFIER
Antibodies		
Mouse anti-NeuN primary antibody	Millipore Sigma	Cat#MAB377; RRID:AB_2298772
Goat anti-mouse Alexa488-conjugated IgG secondary antibody	Invitrogen	Cat#A28175; RRID:AB_2536161
Hoechst nuclear stain	Thermo Scientific	Cat#33342; RRID: AB_10626776
Chemicals, peptides, and recombinant proteins		
N-Methyl-D-aspartate acid >98% (NMDA)	Sigma-Aldrich	Cat#M3262
Cresyl violet Nissl body stain	Electron Microscopy Sciences	Cat#26089-20
Prolong Diamond antifade mountant	Molecular Probes	Cat#P36961
Experimental models: organisms/strains		
Mouse: C57BL/6N	Charles River	RRID:MGI:5651595
Software and algorithms		
Raw data	This paper	Mendeley Data: https://dx.doi.org/10.17632/sspngbxbcz.1
Software and algorithms		
MATLAB 2013b	MathWorks	RRID:SCR_001622; https://www.mathworks.com/products/matlab.html
GraphPad Prism 8	Graphpad	RRID:SCR_002798; https://www.mathworks.com/products/matlab.html
Psychophysics Toolbox	PsychToolbox	RRID:SCR_002881; http://psychtoolbox.org
SPSS v25.0	IBM Inc.	RRID:SCR_002865; https://www.ibm.com/products/spss-statistics
FIJI (ImageJ distribution)	NIH; see reference 78	RRID:SCR_002285; https://imagej.net/Fiji
VEPAnalysisSuite: local field potential analysis suite	Github (Jeff Gavornik, Boston University)	github.com/jeffgavornik/VEPAnalysisSuite
VEPStimulusSuite: visual stimulus generation and presentation suite	Github (Jeff Gavornik, Boston University)	github.com/jeffgavornik/VEPStimulusSuite